Miocene to Recent exhumation of the central Himalaya determined from combined detrital zircon fission-track and U/Pb analysis of Siwalik sediments, western Nepal

Matthias Bernet, Pieter Van Der Beek, Raphaël Pik, Pascale Huyghe, Jean-Louis Mugnier, Erika Labrin, Adam Szulc

Miocene to Recent exhumation of the central Himalaya determined from combined detrital zircon fission-track and U/Pb analysis of Siwalik sediments, western Nepal

MATTHIAS BERNET, PETER VAN DER BEEK

Laboratoire de Géodynamique des Chaînes Alpines, Université Joseph Fourier, BP 53, 38041 Grenoble, France

RAPHAËL PIK

CRPG-CNRS, 15, rue N.D. des Pauvres, BP 20, 54501 Vandoeuvre-Lès-Nancy, France

PASCALE HUYGHE, JEAN-LOUIS MUGNIER, ERIKA LABRIN

Laboratoire de Géodynamique des Chaînes Alpines, Université Joseph Fourier, BP 53, 38041 Grenoble, France

ADAM SZULC

School of Geosciences, The University of Edinburgh, West Mains Road, Edinburgh EH9 3JW, U.K.

Citation: *Bernet, M., van der Beek, P.A., Pik, R., Huyghe, P., Mugnier, J.L., Labrin, E., and Szulc, A., 2006, Miocene to Recent exhumation of the central Himalaya determined from combined detrital zircon fission-track and U/Pb analysis of Siwalik sediments, western Nepal: Basin Research, v. 18, p. 393–412.*

ABSTRACT

Fission-track (FT) analysis of detrital zircon from synorogenic sediment is a well established tool to examine the cooling and exhumation history of convergent mountain belts, but has so far not been used to determine the long-term evolution of the central Himalaya. This study presents FT analysis of detrital zircon from 22 sandstone and modern sediment samples that were collected along three stratigraphic sections within the Miocene to Pliocene Siwalik Group, and from modern rivers, in western and central Nepal. The results provide evidence for widespread cooling in the Nepalese Himalaya at about 16.0 ± 1.4 Ma, and continuous exhumation at a rate of about 1.4 ± 0.2 km/Myr thereafter. The ~16 Ma cooling is likely related to a combination of tectonic and erosional activity, including movement on the Main Central thrust and Southern Tibetan Detachment system, as well as emplacement of the Ramgarh thrust on Lesser Himalayan sedimentary and meta-sedimentary units. The continuous exhumation signal following the ~16 Ma cooling event is seen in connection with ongoing tectonic uplift, river incision, and erosion of lower Lesser Himalayan rocks exposed below the MCT and Higher Himalayan rocks in the hanging wall of the MCT, controlled by orographic precipitation and crustal extrusion. Provenance analysis, to distinguish between Higher Himalayan and Lesser Himalayan zircon sources, is based on double dating of individual zircons with the FT and U/Pb methods. Zircons with pre-Himalayan FT cooling ages may be derived from either non-metamorphic parts of the Tethyan sedimentary succession or Higher Himalayan protolith that formerly covered the Dadeldhura and Ramgarh thrust sheets, but that have been removed by erosion. Both the Higher and Lesser Himalaya appear to be sources for the zircons that record either ~16 Ma cooling or the continuous exhumation afterwards.

Keywords: zircon, fission-track, U/Pb, exhumation, Himalaya, Nepal

INTRODUCTION

The Himalaya has evolved into the currently highest and most impressive mountain belt on Earth since about 50 Ma (e.g. LeFort, 1975). Because of its importance for understanding both continental collision processes, as well as the links and feedbacks between orogenesis and the global climate system (e.g., Raymo & Ruddiman, 1992; Molnar *et al.*, 1993), the

Himalaya has been the subject of several decades of intense research. In spite of this effort, however, many open questions remain about the exhumational history of this classic convergent orogen. Some of the questions that are of interest to us include: What is the recent cooling history of the Himalaya? Has exhumation of the Himalaya in Nepal been continuous or episodic since the mid-Miocene? When did the Himalaya obtain its current elevation? Is the exhumational history of the Himalaya controlled purely by tectonics or can we distill climatic effects?

Because of the rapid exhumation rates encountered in large parts of the Himalayan orogen, *in-situ* low-temperature thermochronological systems, whether they be $^{40}Ar/^{39}Ar$ on mica or feldspar, or zircon or apatite FT, typically yield ages only a few million years old and have no "memory" of earlier events. In order to reconstruct the exhumation history of the Himalaya on longer timescales, we have to turn our attention to the Sub-Himalaya (Fig. 1), where the record of orogenic cooling and exhumation is preserved in the synorogenic sediments of the Siwalik Group, which have been accumulating since the middle Miocene (e.g., Harrison *et al.*, 1993; Burbank, 1996).

In this paper we present a comprehensive study of Siwalik sediments in Nepal using a combination of provenance and thermochronologic analysis, i.e. a FT and U/Pb double-dating technique on single detrital zircon grains, with the aim to shed more light on the timing of cooling and exhumation events or periods, and to improve our understanding of the long-term evolution of the central Himalaya. Twenty-two samples were collected from modern river sediment and Miocene to Pliocene stratigraphic profiles of the Siwalik Group at the Karnali River, Surai Khola, and Tinau Khola sections in western and central Nepal. In addition, two samples were collected from sedimentary units in the Lesser Himalaya, the Tertiary Dumri formation and the Precambrian Khamari Formation in the vicinity of the Main Boundary Thrust in western-central Nepal (Fig. 1).

Detrital zircon fission-track (DZFT) analysis is a well-established tool to study the long-term exhumation history of convergent mountain belts (e.g. Cerveny *et al.*, 1988; Garver *et al.*, 1999; Spiegel *et al.*, 2000; Bernet *et al.*, 2001, 2004a, b). This type of analysis is complementary to the widely applied $^{40}Ar/^{39}Ar$ dating method of white mica, but presents two advantages. First, zircons are common accessory minerals in most clastic sedimentary, metasedimentary, and crystalline rocks in the Himalaya, and they are robust during transport and weathering. Second, the effective closure temperature of the zircon FT system is about 240°C for common orogenic cooling rates of 15°C/Myr (Hurford, 1986; Brandon *et al.*, 1998), and therefore this technique is more sensitive to upper crustal (up to 6-10 km depth) processes, such as erosional and tectonic exhumation, than the $^{40}Ar/^{39}Ar$ system characterized by a closure temperature of 350-420°C, depending on mica type and grain size (von Eynatten & Wijbrans, 2003). In addition, it is possible to combine FT analysis of zircon with other dating techniques, such as U/Pb analysis to better constrain provenance (Carter & Moss, 1999; Carter & Bristow, 2000, 2003). We combine our DZFT data with U/Pb ages obtained on the same zircon grains to constrain the provenance of the DZFT age populations that we recognize. We also compare our DZFT data with $^{40}Ar/^{39}Ar$ ages obtained on detrital white mica from the same sections (Szulc *et al.*, 2006) in order to better confine the exhumational history of the source areas. In a companion paper (van der Beek *et al.*, 2006), we report on detrital apatite FT ages of the same samples to resolve shorter-term variations in exhumation rates as well as the post-depositional thermal history of the Siwalik sediment samples.

GEOLOGIC FRAMEWORK OF THE NEPAL HIMALAYA

Collision of the Indian and Eurasian plates, starting in Paleocene-Eocene times, caused intense crustal shortening and thickening, resulting in the formation of the Himalayan mountain belt and Tibetan Plateau (e.g., Hodges, 2000; Yin & Harrison, 2000). In most studies, the Himalaya is subdivided into four major lithotectonic units, which are the Tethyan Himalayan zone (TH), Higher or Greater Himalayan zone (HH), Lesser Himalayan zone (LH), and the Sub-Himalaya (e.g. Gansser, 1964; Valdiya, 1980; Upreti, 1999). Late Cenozoic north-dipping fault systems, i.e. the South Tibetan Detachment (STD) system, the Main Central thrust (MCT), the Main Boundary thrust (MBT), and the Main Frontal thrust (MFT) bound these lithotectonic units from north to south (Fig.1). The STD is a low-angle normal-fault system, while the MCT is a structurally complex and several km thick thrust zone, and the MBT and MFT are more discrete thrusts (e.g. LeFort, 1986; Yin & Harrison, 2000 and references therein; DeCelles *et al.*, 2001).

The TH is the structurally and topographically highest unit; including some of the highest-elevation Himalayan peaks in Nepal (e.g. Mount Everest, Annapurna). TH rocks consist of Cambrian to Eocene marine sedimentary to low-grade metasedimentary rocks, with local volcanics. These sediments were deposited along the northern margin of the Indian plate prior to continent-continent collision. The Indus-Yarlung suture zone forms the northern boundary of the TH. Structurally below the TH to the south of the STD is the Higher Himalaya, which forms some of the high topography of the Himalayan range. The HH crystalline rocks are made up of Late Proterozoic to early Cambrian metasedimentary rocks, kyanite-sillimanite bearing schist and paragneiss, as well as orthogneiss (e.g. Pêcher, 1989; Schelling, 1992; Hodges *et al.*, 1996). The HH crystallines can be further subdivided into Formations I, II, and III, where Formation I is mainly composed of paragneiss and schist, Formation II consists of paragneiss and calcsilicate gneiss, and Formation III is characterized by orthogneiss bodies that intrude Formation II (e.g., LeFort, 1975; Colchen *et al.*, 1986). Early Miocene tourmaline-bearing leucogranitic plutons have intruded the HH high-grade metamorphic rocks along the STD at around 24-19 Ma (e.g. LeFort, 1981, 1986; Ferrara *et al.*, 1983; Schärer *et al.*, 1986; Guillot *et al.*, 1994, Searle & Godin, 2003).

The Lesser Himalaya is bounded at the base by the MBT and consists mainly of Precambrian clastic sediments and metasedimentary rocks (Brookfield, 1993; Upreti, 1999). One of the interesting aspects of the LH is its inverted metamorphic grade, with lower grade metamorphic rocks to the south, overlain by higher-grade metamorphic rocks to the north, close to the MCT. This upward increase in metamorphism is related to deformation and/or heating in the footwall of the MCT and tectonic imbrication (Pêcher, 1975; Hodges *et al.*, 1996; DeCelles *et al.*, 1998; Stephenson *et al.*, 2000; Pearson & DeCelles, 2005). Bollinger *et al.* (2004) showed in a recent study that peak metamorphic temperatures decrease from ~550°C near the MCT to less than 330°C further to the south within the LH. This change in metamorphic grade is also reflected in a change in $^{40}Ar/^{39}Ar$ white mica ages from 3-4 Ma near the MCT to ~20 Ma near the MBT (Bollinger *et al.*, 2004).

The clastic sedimentary rocks of the early to mid-Miocene Dumri Formation are part of the Himalayan foreland basin deposits and represent the youngest stratigraphic unit of the LH. The 700-1300 m thick fluvial sandstones and red interbedded mudstones of the Dumri Formation were probably derived from erosion of HH and TH rocks (DeCelles *et al.*, 1998; 2004; Robinson *et al.*, 2001).

Thrust sheets, such as the Ramgarh thrust or the crystalline Dadelduhra thrust in western Nepal, are exposed on top of the LH in some areas. The Dadelduhra thrust consists of Precambrian gneiss, mica schist, phyllite, and quartzite, and Late Cambrian to Early Ordovician granitic intrusions, and most workers regard the Dadelduhra thrust sheet as being of Higher Himalayan affinity (e.g. Gansser, 1964; Stöcklin, 1980; Valdiya, 1980; Schelling, 1992). The Ramgarh thrust consists of the Precambrian Kushma and Ranimata Formations, which are primarily made up of quartzites and chloritic-sercititic phyllites respectively (Perason & DeCelles, 2005). These formations are part of the lower Lesser Himalayan meta-sedimentary rocks that experienced upper greenschist facies to lower amphibolite facies metamorphism (DeCelles *et al.*, 1998; Robinson *et al.*, 2003; Pearson & DeCelles, 2005). It is possible that the leading edge of the Ramgarh thrust sheet was emplaced on top of the sedimentary Dumri Formation in the LH during the time of deposition of the lower Siwaliks, at around 15-9.5 Ma (DeCelles *et al.*, 1998; Robinson *et al.*, 2001, 2003; Huyghe *et al.*, 2005; Pearson & DeCelles, 2005).

The Sub-Himalayan thrust belt is bounded by the MBT to the north and the MFT to the south (Fig. 1). The Sub-Himalaya is made up of the clastic Siwalik Group, which consists of at least 4-5 km thick middle Miocene to Pliocene siliciclastic foreland basin sediments that were incorporated into the Sub-Himalayan thrust belt in the last few million years (Mugnier *et al.*; 2004).

Sedimentology and stratigraphy of the Siwalik Group

The fluvial deposits of the Siwalik Group are informally subdivided into the lower, middle and upper Siwalik sub-groups based on lithostratigraphy (e.g., Quade *et al.*, 1995). Stratigraphic ages of the Siwalik Group range between ~15 and 1 Ma, and were determined by the means of magnetostratigraphic correlations (Appel *et al.*, 1991; Gautam & Rösler, 1999; Gautam & Fujiwara, 2000; T.P. Ohja, pers. commun. 2003), and vertebrate fossils (West *et al.*, 1978; Corvinus & Rimal, 2001). The Siwaliks are characterized by five fluvial lithofacies consisting of sandy channel, gravelly channel, crevasse splay, flood plain, and paleosol deposits (DeCelles *et al.*, 1998; Nakayama & Ulak, 1999; Huyghe *et al.*, 2005), and show an overall coarsening upward trend (Fig. 2). Flow directions measured within the Siwalik sediments are consistently toward the south, indicating transverse transport similar to the modern drainage pattern in the northern Ganges flood plain (DeCelles *et al.*, 1998; Szulc *et al.*, 2006). The lower Siwaliks in western Nepal were deposited between ~15 and 8-10 Ma. They consist of channel sandstones interbedded with overbank mudstones in which oxidized calcitic paleosols are developed. The middle Siwaliks, deposited between 8-10 and ~3.5 Ma, are made up of stacked sandy channel sandstones and 0.05 – 1.5 m thick drab-colored histosols. The channel deposits can be up to 20 m thick. The upper Siwaliks are in general gravelly braided river sediments, which commonly display clast imbrication, and alluvial fan deposits (DeCelles *et al.*, 1998; Nakayama & Ulak, 1999; Huyghe *et al.*, 2005). These sediments were deposited between ~3.5 and 0.5 Ma. The Siwalik sedimentary rocks are tilted and thrusted, and are generally well exposed along rivers such as the Karnali, Surai and Tinau, which currently incise into them. The MFT bounds the Siwalik Group to the south, where it overlays Quaternary gravels of the northern Indo-Gangetic plain (e.g. Nakata, 1989; Schelling, 1992; Mugnier *et al.*, 1993, 2004).

Sources for Siwalik Group sediments

Provenance studies for the Siwalik Group sediments (cf. Najman, 2006 for a review) have mainly concentrated on petrography and heavy-mineral analyses (DeCelles *et al.*, 1998; White *et al.*, 2002; Szulc *et al.*, 2006), Sr and Nd isotopes (Huyghe *et al.*, 2001, 2005; Robinson *et al.*, 2001) and U/Pb ages of zircons (DeCelles *et al.*, 1998). These methods can be applied because the different lithotectonic units of the Himalayas have distinctive isotopic (France-Lanord *et al.*, 1993; Ahmad *et al.*, 2000) and geochronological (Parrish & Hodges, 1996; DeCelles *et al.*, 2000, 2004) signatures. Specifically, zircons derived from the TH sequence have characteristically young U/Pb ages with peaks at ~500 and 1000 Ma, while HH zircons are broadly clustered around 1100 Ma, with minor peaks at ~1500-1700 and ~2500 Ma (DeCelles *et al.*, 2000, 2004). Granitic gneisses of Formation III in the HH, as well as undeformed granitic rocks in the klippen covering the LH, yield zircons with U/Pb ages of around 500 Ma (DeCelles *et al.*, 2000, 2004). The silicate fractions of HH rocks have mean ε_{Nd} values of approximately -15‰, and TH rocks are only subtly different, showing a somewhat larger negative range. The LH is clearly distinct with ε_{Nd} values of around -23‰ and a U/Pb age distribution of zircons peaking at ~1800 and ~2500 Ma (DeCelles *et al.*, 1998, 2000, 2004; Ahmad *et al.*, 2000; Robinson *et al.*, 2001).

Petrographic modes of the Siwalik sandstones imply that they contain detritus from sedimentary and low-grade metamorphic origin, with the proportion of K-feldspar, plagioclase, and metamorphic minerals increasing upward (DeCelles *et al.*, 1998; White *et al.*, 2002; Szulc *et al.*, 2006). An up-section decrease in ε_{Nd} values observed in the Karnali, Surai Khola, and Tinau Khola sections (Huyghe *et al.*, 2001), together with an increase in zircons older than 1500 Ma (DeCelles *et al.*, 1998) suggests a growing contribution from LH source rocks to the Siwalik detritus since ~13 Ma. Nevertheless, kyanite is always present in the heavy mineral fraction of Siwalik sandstones, indicating a consistent sediment input from higher-grade metamorphic rocks throughout the depositional history of the Siwaliks.

DETERMINING EXHUMATION USING DETRITAL ZIRCON FT THERMOCHRONOLOGY

Studying cooling ages of detrital grains from synorogenic sediments provides the unique opportunity to obtain information about exhumation rates in the past (e.g. Cerveny *et al.*, 1988; Garver & Brandon, 1994; Garver *et al.,* 1999; Spiegel *et al.,* 2000; Bernet *et al.,* 2001). The bedrock that was exposed at the surface in the Himalaya during the Miocene and Pliocene has been eroded, but the cooling-age signal is preserved in the Siwalik Group. Central to detrital FT thermochronology is the concept of lag time, defined as the thermochronological age minus the depositional age (e.g. Garver *et al.*, 1999; Bernet *et al.,* 2001); the concept is explained in Figure 3. For determining past exhumation events or periods of a convergent mountain belt such as the Himalaya, the task is A) to obtain samples from the bottom to the top of stratigraphic sections of foreland basin deposits, B) to date individual zircons from each sample and decompose the observed grain-age distributions into major peaks by binomial peak fitting or other statistical means, and C) to interpret the results in terms of length of lag time and how peak ages change up-section (Fig. 3C).

There are some crucial aspects for this kind of analysis. First, it is of advantage if no acidic volcanism is present in the study area contemporary to the time of deposition of synorogenic sediments, because volcanic zircon with young FT ages could swamp the system, masking orogenic cooling ages (see review by Bernet & Garver, 2005 and references therein). Second, it is very important that the depositional age of the studied strata is reasonably well known (±1 Myr), to be able to apply the lag-time concept. In the case of the Siwalik Group, depositional ages are well controlled by magnetostratigraphy (e.g. Gautam & Rösler, 1999; Gautam & Fujiwara, 2000; T.P. Ohja, pers. commun. 2003; cf. van der Beek *et al.*, 2006 for a discussion of the magnetostratigraphic dating of our sections), and ongoing volcanic activity is no concern in the Himalaya. Consequently, the lag-time concept can be applied in this study to reconstruct the recent cooling history of the central Himalaya. A third important aspect that needs to be considered is that post-depositional burial and heating can cause partial or full resetting of FT ages. It is therefore useful to obtain independent estimates on burial temperature, such as from vitrinite reflectance. However, because of the relatively high temperature range for zircon FT annealing (~200-250°C, depending on the degree of α-damage and heating duration, Brandon *et al.*, 1998), this would only be a concern for the most deeply buried samples in the Himalayan foreland basin and in those samples not even the apatite FT ages are totally reset (van der Beek *et al.*, 2006).

A sample of detrital zircon nearly always contains a range of cooling ages, which belong to different grain-age components or peaks (Fig. 3B). The reason for this is that different sources in a mountain belt (FT source terrains), characterized by individual cooling histories, contribute zircons to synorogenic sediment. The only exception from this rule may be small drainages that sample only a single FT source terrain. By looking at the distribution of bedrock FT ages on an orogenic scale there seems to be no continuous change in FT ages across the landscape. Instead, bedrock FT ages tend to cluster in specific age groups, which can be recognized as FT age peaks in detrital samples (see example of the European Alps by Spiegel *et al.*, 2000; Bernet *et al.*, 2001, 2004 a, b).

Because lag time integrates between the time when zircons cool below the effective closure temperature of the FT system and the time when they are deposited in foreland basin sediments, it can be transferred into a long-term average exhumation rate (Garver *et al.*, 1999), given that temporary storage of detrital material in intermontane basins or fluvial systems during transport is considered negligible. This is commonly the case in active orogenic systems, so transport time can be regarded as geologically instantaneous (Bernet *et al.*, 2004a). The cooling ages determined in the detrital samples are therefore representative of erosional and tectonic exhumation, which are linked to the climatic and tectonic history of the source region.

Once the zircons are dated and the peak ages in each sample have been determined the up-section evolution of peak ages and associated lag times can be analyzed (Fig. 3). In general there are three main possibilities. First, the peak ages are constant and the lag time correspondingly increases continuously up-section. This situation is termed a static peak (Garver & Brandon, 1994; Bernet & Garver, 2005); zircons belonging to such a peak are either A) derived from a source area that experienced a rapid but short-lived cooling event, B) recycled from a sedimentary source, in particular if the peak age is relatively old and pre-dates orogenesis, or C) result from the erosion of thick sections of non-reset volcanic rocks (e.g., Ruiz *et al.*, 2004). Second, the peak age becomes younger up-section; this scenario is known as a moving peak (Garver & Brandon, 1994; Bernet & Garver, 2005). Peak ages that young at the same rate at which the depositional age changes, leading to an approximately constant lag time, are an indication for continuous exhumation at a constant rate (Bernet *et al.*, 2001; Willett & Brandon, 2002; Bernet & Garver, 2005). Peak ages may also become younger up-section at a rate faster than the depositional age, which leads to a shortening in lag time indicating acceleration in exhumation in the source area over time.

On the basis of these rather simple lag-time trends, the overall long-term average exhumation history of a mountain belt can be determined. For analysis of short-term variations in exhumation rates (on the 10^5-year scale) other dating methods, with closure temperature isotherms closer to the surface, such as apatite (U-Th)/He or FT, are needed. Nonetheless, these techniques have the risk that grains are more easily partially or fully reset after deposition, losing their signal of source-area exhumation (cf. van der Beek *et al.*, 2006).

It is important to keep in mind that exhumation, bringing rocks closer to the surface, can be driven by both surface erosion and tectonic exhumation. Normal faulting leads to rapid cooling of footwall rocks; the recorded cooling rate is in this case related to the slip rate on the fault, which may occur either episodically or continuously. Tectonic activity on thrust faults does not exhume or cool rock in itself, because overlying material in the hanging wall is not removed by the thrusting. However, rocks may be removed by contemporaneous erosion at the surface of the thrust sheet, which will cause cooling. Exhumation and cooling of rock are thus very closely related. Slow exhumation of rock will cause slow cooling and long lag times. Fast exhumation will cause fast cooling, but it may also cause advection of isotherms, which are compressed toward the surface, increasing the thermal gradient (Stüwe *et al.*, 1994). If fast exhumation is continuous, then the thermal structure of the orogen will adjust to a new steady-state thermal profile within a few million years (e.g., Batt & Braun, 1997). If fast exhumation is short-lived, then the isotherms will eventually relax, leaving behind a thick upper-crustal section with relatively homogeneous cooling ages. Erosion of zircon from such a crustal section leads to a static FT age peak in the detrital record. Ongoing incision by rivers and glaciers will sooner or later cut into and expose deep-seated bedrock with erosion-related cooling ages, resulting in a moving FT age peak in synorogenic sediments. Topographic relief can have an effect on thermochronologic systems with lower closure temperatures, such as apatite FT or (U-Th)/He dating, but is less a concern for the zircon FT system, especially if the wavelength of the relief is <10 km.

DATING METHODS

In this study we used the external detector method to determine zircon FT ages (e.g. Wagner & Van den haute, 1992). For each sample, aliquots of zircon were mounted in Teflon®, polished to expose internal grain surfaces, and etched in a eutectic NaOH-KOH melt at 228°C in a laboratory oven. Etch times ranged between 15 and 40 hours. If enough sample material was available, at least two mounts were prepared per sample and etched for different lengths of time, to ensure that the full spectrum of datable grains was covered (Naeser *et al.*, 1987; Garver *et al.*, 2000; Bernet *et al.*, 2004b). All samples were covered with low-uranium muscovite as the external detector and irradiated together with Fish Canyon Tuff and Buluk Tuff age standards, and CN1 dosimeter glasses at the well-thermalised ORPHEE reactor in Gif-sur-Yvette, France. FT ages were calculated using the zeta-calibration method (Hurford, 1998), and major grain-age peaks in each sample were determined using the binomial peak-fitting approach based on the work by of Galbraith & Green (1990), outlined in Brandon (1996) and Stewart & Brandon (2004). All FT dating was done in the FT laboratory at Grenoble, France.

Almost no bedrock zircon FT ages exist for the Tethyan, Higher, and Lesser Himalaya in western and central Nepal, which would allow comparison with DZFT grain-age distributions. However, a wealth of both bedrock and detrital zircon U/Pb data exist for western and central Nepal, and is it has been repeatedly shown that the major lithotectonic units have distinct zircon U/Pb age spectra (e.g. DeCelles *et al.*, 1998, 2000, 2004; Amidon *et al.*, 2005a and b). By combining FT and U/Pb dating on the same individual grains the provenance of these grains can be distinguished between TH, HH and LH sources.

A total of 61 single zircons from samples KA-UP, SUR 20, SUR 17, and SUR 8, which were dated with the FT method, were also analyzed with the U/Pb method, using a Cameca IMS 1270 ion microprobe at the CRPG in Nancy, France. All zircon grains remained in their Teflon® mounts after FT analysis and photographic maps were produced for each mount on which grains dated with the FT method were marked. These maps were used to locate the same grains after loading the mount in the ion probe for U/Pb analysis. Parts of the 91500 standard zircon from Ontario (Canada), with an age of 1,062 +- 0.4 Ma (Wiedenbeck *et al.*, 1995), were also mounted in Teflon® and loaded in the ion microprobe with the sample mounts. Point analyses on this standard were performed after each measurement of three zircon grains. The standard was also used to calibrate the ages after measurement of $^{196}Zr_2O$, ^{204}Pb, ^{206}Pb, ^{207}Pb, ^{208}Pb, ^{238}U, ^{248}ThO and ^{254}UO (see details in Deloule *et al.*, 2002). The spot size of the ion microprobe varied between 30 x 40 and 40 x 50 μm, with the beam of the ion microprobe being positioned in the center of each grain. Because the measured zircons were generally small (diameter <100 μm), and because they were polished up to the core of the grains, we can consider that the measured ages represent a mean of the various potential age zonation generally present in such old polymetamorphic minerals. Correction for common lead was made using the ^{204}Pb amount and applied to the $^{207}Pb/^{206}Pb$ age following the Stacey and Kramer's (1975) model.

RESULTS

Fission-track analysis

In general, it is our goal to date at least 50-100 grains per sample to obtain statistically robust results when the observed grain-age distribution is decomposed into major grain-age components or peaks (e.g. Brandon, 1996; Stewart & Brandon, 2004). Unfortunately, statistical analyses had to be done on less than 50 grains in many samples due to relatively poor zircon yield. Nevertheless, because of the clear separation of grain-age components, we are confident with the results. Figure 4 gives an example of the observed grain-age distribution and the binomial fitted peaks of a detrital sample; in this case modern sediment from the Karnali River in western Nepal, for which at least four main FT peaks can be distinguished at about 4.0 ± 1.1, 9.3 ± 1.3, 19.1 ± 3.0 and 216.6 ± 135.7 Ma. The age range of dated grains and binomial fitted peaks for all other Siwalik samples are given in Table 1. All of the Siwalik samples failed the χ^2 test, indicating that the grains were derived from multiple sources. Despite the fact that some samples have individual grains with FT ages close to or slightly younger than the depositional age, no indications were found for partial resetting of zircon within the Siwalik Group. Therefore, temperatures within the Siwalik sediments remained well below 200°C (Brandon *et al*., 1998; Garver *et al*., 2005; Bernet & Garver, 2005). This is consistent with the observation that apatite FT ages are not completely reset even for the deepest samples, as well as with vitrinite reflectance (R_0) values ≤1 % throughout the sections (cf. van der Beek *et al*., 2006). Thus, the DZFT ages unambiguously carry a source-area exhumation signal.

Our Siwalik samples are characterized by 2 or 3 main DZFT-age peaks (Table 1), which can be summarized in three peak-age groups (Fig. 5). Each sample contains grains that belong to an old peak with FT ages between 80-150 Ma, and a much younger peak, which has on average a 16.0 ± 1.4 Ma age (Karnali section 15.8 ± 1.8 Ma, Surai Khola section 16.1 ± 1.5 Ma, Tinau Khola section 15.9 ± 0.9 Ma, based on >340 single zircon FT ages belonging to this peak). Both, the 80-150 Ma and ~16 Ma peaks, are fairly consistent and do not change significantly up-section, therefore, they can be considered as static peaks. Typically, 20-35% of the dated zircons fall into the old static age-peak; whereas 35-95% of the grains make up the younger static peak (Table 1; Figure 5b). From about 11 Ma to the present an even younger peak can be detected, containing 5-45% of dated zircon grains. This peak changes in age up-section (moving peak), retaining a relatively constant lag-time of ~4 Myr, although it is noteworthy that the size of this peak seems to progressively decrease up-section (Table 1). The modern Karnali River sample, with a relatively rich zircon yield, also shows an intermediate 9 Ma age group between the moving peak and the young static peak.

For the two samples collected in the LH near the MBT only 13-14 grains per sample were dated, because the principle objective was to constrain whether these samples were fully reset either during burial or during emplacement of the Ramgarh thrust onto part of the Tertiary sediments of the LH. Sample BIR 1 was collected from the stratigraphically lower part of the early-mid Miocene Dumri formation at a location just 380 m north of the MBT, while sample SUR 23 is from the Precambrian Khamari formation, collected from a location 400 m north of the MBT. Both samples show a significant spread in ages, with minimum ages of ~15 Ma, which is somewhat younger than the depositional age of about 20 Ma for the Dumri formation at this location (e.g. DeCelles *et al.*, 2004), and much younger than the depositional age of the Khamari formation. Both samples also contain older grains with ages between 50-90 Ma (Fig. 6, Table 2).

Single zircon FT-U/Pb analysis

As mentioned above, 61 single zircons, for which FT ages were determined, have been analyzed with the U/Pb method (Fig. 7; Table 3). This was done to constrain zircon provenance between TH, HH, and LH sources on the basis of U/Pb ages, by comparison with published bedrock and detrital zircon data (Parrish & Hodges, 1996; DeCelles *et al.* 1998, 2000, 2004). A large proportion of dated grains fall close to the concordia line, as shown in Figure 8. In this case the ages can be interpreted as the age of crystallization of the zircons. However, some of the zircons which plot on the right side of the concordia line show clear evidence of Pb loss and define some trends of discordance with a common early Paleozoic lower intercept and various old (2Ga to 3Ga) upper intercepts. Because it could be ambiguous to interpret such trends (inheritance of old recycled cores or simple partial thermal resetting) we decided to follow the same criteria used by DeCelles et al. (2004) and we do not take into account ages which were more than 30% discordant. Therefore, the age we retained and plotted on Fig. 7 as the "U/Pb age", is: the $^{238}U/^{206}Pb$ age in case all the ages were concordant and the $^{207}Pb/^{206}Pb$ age in case of slight discordance.

The distribution of the U/Pb ages for the zircons measured in our study (Fig. 7) is fairly comparable to the distribution obtained by other authors (e.g. DeCelles et al., 2004) on a larger number of grains. The peaks of the different Himalayan tectono-stratigraphic units are clearly separated and can be easily recognized at: 400-1200 Ma for the HH and TH, 1500-2100 Ma for the LH, and a common HH-LH-TH peak at about 2500 Ma.

The results of this combined dating approach, illustrated in Fig. 7, allow proposing some important constraints concerning the provenance of zircons belonging to the various DZFT peaks, previously identified with the FT data set (Fig. 5). First, grains falling within the 80-150 Ma old static peak tend to have relatively young U/Pb ages of 500-1000 Ma whatever their depositional age. Concerning, the ~16 Ma static peak and the younger moving peak (4 Myr. lag time), it seems that the age of the grains are equally distributed in the LH and in the HH age-ranges for the present day (KAR-up) and the two most recent sandstone samples SUR-20 and SUR-17, with depositional ages of 1 and 4 Ma respectively. To the contrary, the age distribution of zircons from the 7 Ma sandstone SUR 8 define two distinct and restricted groups: zircons which belong to the ~16 Ma static peak exhibit LH, HH and TH ages, whereas zircons from the younger moving FT peak are characterized by U/Pb ages typical of the HH.

DISCUSSION

In the introduction of this paper we posed questions concerning the exhumation and cooling history of the Himalaya in Nepal. By using the zircon FT method we are able to determine the history of cooling from about 240°C, which corresponds to a crustal depth of approximately 6-10 km, depending on local geothermal gradients. Therefore, we can neither resolve deep crustal processes, nor will we detect very short-term variations in erosion rates. But we are able to determine the long-term, over millions of years, average exhumation rate of the upper crust of the Himalaya in western and central Nepal. Given this framework, what is the exhumational signal that we find in detrital zircon from modern river sediment and mid-Miocene to Pliocene Siwalik Group deposits? In order to facilitate the later discussion on the geodynamic significance of the different age groups identified, we will first investigate whether they can be unambiguously attributed to different source areas.

Combined FT and U/Pb zircon provenance analysis

The combined FT-U/Pb single grain dating experiment provided us two important results:

1) Most of the double-dated zircons from the "old" (80-150 Ma) static peak have U/Pb ages between 500-1000 Ma; three grains have U/Pb ages of 1800-2400 Ma (Fig. 7). The combination of pre-Himalayan DZFT ages and late Proterozoic-Paleozoic U/Pb ages would point to a TH source for these zircons. Even if this is our preferred interpretation, we have to acknowledge that the currently exposed Lower Mesozoic Tethyan sedimentary succession in central northern Nepal may have experienced temperatures of 200-250°C, whereas the Paleozoic succession has been metamorphosed at temperatures >300°C, based on illite crystallinity, organic thermal indicators, and rock-magnetic properties (Garzanti *et al.,* 1994; Crouzet *et al*., 2001). Such temperatures would lead to partial or full annealing of fission-tracks in zircon and no >100 Ma cooling ages would be preserved. Only the overlying Upper Mesozoic sedimentary succession in the TH would yield pre-Himalayan ZFT ages, but few erosional remnants of these rocks are currently preserved. Another possible source region for these zircons would be sedimentary HH protolith material from non-metamorphic nappes that would have overlain the crystalline HH but have now all but been eroded away. A similar source has been invoked by White *et al.* (2002) and Szulc *et al.* (2006) to explain the sedimentary detrital input into the western Indian and western Nepal Siwaliks, respectively. The three grains with older U/Pb ages between 1800-2400 Ma may be recycled zircons from Lesser Himalayan sedimentary rocks (e.g. Dumri and other Tertiary formations), although paleo-Proterozoic U/Pb ages are also reported from the TH sediments (DeCelles *et al*., 2004).

2) The two young DZFT age peaks are not clearly separated with respect to zircon U/Pb provenance. Zircons belonging to both the ~16 Ma static peak and the 4 Myr lag-time moving peak spread the full range in U/Pb ages from ~500 to ~2500 Ma, although neo-Proterozoic U/Pb ages appear slightly under-represented in the young static peak (Fig. 7). Because of the complexity of the U/Pb age-structure of especially the HH crystallines, it is not possible to infer firm conclusions from these data. Nevertheless, taking into account that zircon yield from HH rocks maybe 2-4 times that from LH lithologies (Amidon *et al.*, 2005a), it appears that grains belonging to the ~16 Ma static peak are derived from both HH and LH sources (Fig. 7), and possibly preferentially from the latter, because the exposed area of LH rocks increased over time. With the currently available dataset it is not possible to determine how much of the material in the two static peaks was recycled from Tertiary foreland basin

sediments when they were incorporated into the fold-and-thrust belt during the deposition of the Siwalik Group from the mid-Miocene on.

The unexpected result of this double-dating exercise is that grains belonging to the 4 Myr lag-time moving peak also appear to be derived from both the HH and LH, even though one could probably argue that the observed U/Pb age spectrum for this group is also consistent with a HH source alone, as it seems to be the case for sample SUR8, which was deposited at 7 Ma (Fig. 7). However, recognizing again the important difference in zircon yield between HH and LH sources and the relatively high proportion of ~1800 Ma (main LH peak) ages, we prefer the interpretation that in general both sources contributed zircons to this peak. The most likely source region for these zircons lies in the area around the MCT, where both HH and LH zircons may have experienced a similar recent low-temperature cooling history and from where ~4 Ma young $^{40}Ar/^{39}Ar$ ages were reported as well (Bollinger *et al.*, 2004). The implications of this inference will be discussed below.

Geodynamic significance of DZFT age peaks

For discussing the FT age peaks, let us start with the oldest recurring static peak in each sample, which in general ranges between 80-150 Ma (Fig. 5, Table1). This peak contains zircon with non-reset pre-Himalayan cooling ages or possibly partially reset zircons. As argued above, these zircons are likely derived from sedimentary rocks from the TH or previously overlying the HH, which have been all but eroded away. In addition there may be some input of recycled grains from the Lesser Himalayan sedimentary rocks from 7 Ma on (Huyghe *et al.*, 2005). The consistent occurrence of this peak, with a size of ~20-35% in all samples requires a continuous supply of zircons from these sources, or significant recycling of the Tertiary foreland basin deposits. With the zircon FT and U/Pb data we are not able to determine how much recycling occurred within the Siwalik deposits, but apatite FT data presented in the companion paper show that for the most recent samples in the Surai Kohla section such recycling can be recognized (van der Beek *et al.*, 2006).

The young static peak of ~16 Ma reflects synorogenic cooling in the Himalaya, just before deposition of the Siwalik Group started in the foreland basin. The ubiquitous occurrence of this peak throughout the Siwalik sediments, as well as its age, is broadly consistent with the occurrence of a minimum-age peak of ~15-20 Ma observed systematically in the detrital white mica $^{40}Ar/^{39}Ar$ data of Szulc *et al.* (2006), as well as with a similar peak observed in a study of Dharamsala (Dumri equivalent) and Siwalik sediments in western India by White *et al.* (2002), or in modern river sediment of the Marsyandi drainage system in central Nepal by Brewer *et al.* (2003) and Ruhl & Hodges (2005).

The origin of a pulse of synorogenic cooling around 16 Ma

The continuous influx of zircons with ~16 Ma FT and white mica with 15-20 Ma $^{40}Ar/^{39}Ar$ cooling ages requires an explanation. Different possibilities can be considered, including a) contribution of zircon from Miocene leucogranites, b) cooling of zircon and mica related to movement on major faults and thrusts associated with erosion between 15 and 20 Ma, or c) fast cooling in response to surface uplift and fast erosional exhumation, starting around 18 Ma. All three possibilities will be discussed below.

Miocene Leucogranites

The simplest scenario or source of zircon with ~16 Ma cooling ages is that they are derived from the Miocene leucogranites that can be found throughout the Himalaya. These leucogranites are known to have intruded HH metamorphic rocks around 22-24 Ma in Nepal and were then rapidly exhumed between 16 and 19 Ma, which Guillot *et al.* (1994) attributed to tectonic exhumation. We do not yet have direct zircon FT ages from outcrops of leucogranites in Nepal (FT analysis of zircon from the Manaslu leucogranite is currently being prepared), but the Shivling and Kinnaur Kailash granites in the Garhwal Himalaya, western India, yield ZFT ages of 9-14 Ma, and 13-16 Ma, respectively (Searle *et al.*, 1999; Vannay *et al.*, 2004). In Nepal, the cooling histories of these intrusions are well established from other thermochronologic analyses and are summarized in Figure 9 (data from Deniel *et al.*, 1987; Copeland *et al.*, 1990; Guillot *et al.*, 1994). This synthesis suggests a cooling rate of about 50°C/Myr, resulting in an estimated zircon FT cooling age of ~16 Ma for the leucogranites, taking into account a FT closure temperature of ~250°C for the given cooling rate. However, these granites yield zircons with discordant U/Pb ages with Paleozoic upper- and Miocene lower-age intercepts (e.g., Hodges *et al.*, 1996). We have encountered no such U/Pb ages in our analyzed zircons. Although the zircons showing most discordant U/Pb ages belong to the young DZFT age groups, the upper-age intercepts for these samples are consistently ≥ 2000 Ma. It thus seems that the contribution of zircon from leucogranites to Miocene-Pliocene Siwaliks and modern river sediment is very limited, and such zircons may not be detected in our detrital samples. Amidon *et al.* (2005a and b) document a similar result of extraordinarily low zircon contribution from the Miocene leucogranites in modern sediment.

Movement on major fault systems

Widespread rapid cooling at ~16 Ma may be related to movement on some of the major fault systems in the Himalaya. Movement along the MCT and associated cooling below 300-450°C has been documented to have occurred ~20-22 Ma (Hubbard & Harrison, 1989; Copeland *et al.,* 1991; Harrison *et al.*, 1992; Macfarlane *et al.*, 1992; Macfarlane, 1993; Coleman, 1996; Kohn *et al.*, 2001), as well as movement along the STD between ~21 and 16 Ma (Burchfiel *et al.*, 1992; Hodges *et al.*, 1996; Coleman, 1996). Contemporaneous movement of MCT and STD may have caused crustal extrusion of HH rocks, as argued by Beaumont *et al.* (2001), Hodges *et al.*, (2001), and Grujic *et al.* (2002), which predicts rapid cooling, but would provide grains with HH U/Pb ages only. If the ~16 Ma FT cooling-age peak is related to MCT movement, then it can only be regarded to represent the late stages of post-movement cooling.

Movement along other major thrust faults, such as the Ramargh thrust, also occurred during middle Miocene times, passively carrying HH rocks in the overlying crystalline Dadeldhura thrust sheet over LH rocks (DeCelles *et al.*, 2001; Robinson *et al.*, 2003; Pearson & DeCelles, 2005). The MCT and Ramgarh thrust faults were tilted and deformed through growth of the LH duplex structure, starting in the late Miocene, attributed to continuous convergence and crustal shortening (Fig. 10). Useful discussions and summaries of the succession of deformational events and movement of individual thrusts in Nepal are given by Robinson *et al.* (2003), Huyghe *et al.* (2005), and Pearson and DeCelles (2005). Of interest for us is that the emplacement of the Ramargh thrust sheet onto the sedimentary units of the Lesser Himalayas took place during 11-18 Ma (e.g. DeCelles *et al.*, 1998, 2000; Robinson *et al.*, 2001, 2003).

The samples we dated from sedimentary units in the Lesser Himalaya in proximity to the MBT show both a peak at ~15 Ma, which is younger than the depositional age of these samples, but they also contain zircons with much older cooling ages that are either not reset at all or possibly only partially reset. The FT ages of individual grains from these samples are plotted against the uranium content in Figure 6. The displayed pattern is typical for a fraction of low retentive zircon (LRZ) with generally higher uranium content than the non–reset or partially reset grains in the same sample (Garver *et al.*, 2005). Zircons in these samples had accumulated different amounts of α-recoil damage prior to emplacement of the crystalline thrust sheet, given their previous cooling histories and their uranium concentrations. Grains with higher uranium (and thorium) content will accumulate significantly more α-damage than grains with lower uranium content over long periods of time (e.g. 50-100 Myr), and grains with higher amounts of α-damage (LRZ grains) are more easily reset at lower temperatures (see Garver *et al.*, 2005 for further discussion). Therefore, in the southern part of the Lesser Himalaya some detrital zircons were totally or partially reset and others not. At this stage it is not clear if the resetting is the consequence of sedimentary burial, or if it occurred during emplacement of thrust sheets on top of LH rocks. With just 800-1300 m thickness of the Dumri formation in western Nepal (DeCelles *et al.* 1998, 2004) it is difficult to explain resetting of zircon even at the deepest stratigraphic level in this formation, if a regular thermal gradient of 20-30°C is assumed for the foreland basin. However, sedimentary burial may be a plausible explanation for the stratigraphically underlying Khamari formation sample, but it is not known how deep the sample was once buried. A second possibility for resetting is that LH sedimentary rocks were heated during emplacement of hot thrust sheets onto them. This scenario has at least been described by Sakai *et al.* (1999), who reported metamorphic overprint of pre-Siwalik foreland basin sediments below the Kuncha-Naudanda thrust sheet in Western Nepal. These authors report a 16.64 ± 0.47 Ma $^{40}Ar/^{39}Ar$ muscovite cooling age from the Dumri formation to specify the timing of the metamorphic overprint. This would fit with the 15 Ma reset zircon FT peak we found in our samples, indicating fast heating during thrust emplacement and rapid cooling afterwards. The problem with this interpretation is that this type of metamorphic overprint of the Dumri formation has not been reported elsewhere (e.g. DeCelles et al. 1998, 2004). In most reconstructions of thrust movements in the Nepalese Himalayas it is argued that movement of the Ramgarh thrust started around 15-16 Ma, maybe as early as 18 Ma, but by 15 Ma the thrust sheet had not advanced far to south yet, into the proximity of the future MBT. Obviously, this apparent time-paradox of burial, thrust movement, resetting, and exhumation of LH sedimentary rocks needs further detailed attention. So far we can only say that whatever caused heating and resetting of the LRZ in the Lesser Himalayan sedimentary rocks, it was not sufficient to reset all zircons. Consequently, heating was not in excess of 200-220°C for any geologically significant amount of time. Subsequent cooling, which started at 15 Ma, given by the reset peak in both samples, was most likely caused by erosion of overlying material in the area where the samples were collected, and this may in fact be a consequence of or related to the next point of our discussion

Rapid surface uplift around 18 Ma?

The third possibility that we need to consider is that the ~16 Ma static FT peak in the Siwalik samples relates to accelerated surface uplift in the Himalaya. One possible scenario is that rapid surface uplift was caused by slab break-off of Indian lithosphere at around 18 Ma (Mugnier & Huyghe, 2006). Slab break-off would cause isostatic rebound of the orogenic system, which in turn would result in surface uplift (Buiter *et al*., 2002). Surface uplift by itself does not necessarily cause cooling, but it will trigger faster erosion by creating relief as well as enhancing orographic precipitation (Willett, 1999; Willett & Brandon, 2002). Fast erosion in turn will cause advection of relatively shallow isotherms upwards, and incision of rivers and glaciers will lead to the development of high relief and compression of isotherms under valleys. Eventually isotherms will achieve a new equilibrium for the given topography, relief, mean elevation, and average exhumation rate, and create a stable thermal structure of the orogen (e.g. Beaumont *et al.,* 1999; Willett, 1999; Willett & Brandon, 2002).

In-situ bedrock ZFT ages for the Higher Himalaya in central Nepal, as reported by Arita & Ganzawa (1997), are ≤2.5 Ma, indicating that post-middle Miocene exhumation rates in the HH were too high to preserve crustal material recording such an 18 Ma event. Similarly young ZFT ages have been reported from the HH in Western India (Jain *et al*., 2000). No *in-situ* ZFT ages have been reported for the LH, except for our data discussed above, but we note that mica $^{40}Ar/^{39}Ar$ ages are relatively constant at ~17-20 Ma up to 30 km north of the MBT in central Nepal (Bollinger *et al*., 2004). This frontal part of the LH may thus provide a large portion of the ~16 Ma DZFT age-peak, which is both consistent with the indication in the U/Pb ages and with the increasing relative importance of this peak up-section, corroborated by Nd-isotopic evidence for an increasingly important LH source (Huyghe *et al*., 2001; Robinson *et al*., 2001). Thus, the frontal LH may preserve the thermochronological evidence for a dramatic pulse of uplift and exhumation in the middle Miocene.

Evidence for continuous exhumation since Late Miocene times

To finish the discussion on peak ages, let us turn our attention to the moving peak age group, which continuously changes up-section while retaining a fairly constant lag time of ~4 Myr This peak becomes clearly separated from the ~16 Ma static peak at ~11 Ma (Fig. 5), but it is noteworthy that the 4 Myr lag time can possibly be traced back until 14 Ma, however, between 14 and 11 Ma the moving peak cannot be distinguished from the static peak. Considering that the 4 Myr lag time clearly appears at 11 Ma means that constant exhumation started at around 15 Ma, just following the widespread ~16 Ma cooling. The constant 4 Myr lag time can be translated into a long-term average exhumation rate of at least 1.4 ± 0.2 km/Myr, assuming a thermal gradient of less than 40°C/km (Garver *et al.*, 1999; cf. van der Beek *et al.*, 2006, for details on the calculation). The source of the zircons in the moving peak must be deep-seated rock that has been exhumed possibly by a combination of continuous river incision and/or glacial scouring at the surface, and tectonic exhumation. Such exhumation delivered zircons with progressively younger cooling ages, marking a moving peak in the detrital record since the mid-Miocene. Plausible sources for these young zircons are therefore in the southern HH and the northernmost LH, areas that are characterized by *in-situ* ZFT and mica $^{40}Ar/^{39}Ar$ ages of a few Ma (Arita & Ganzawa, 1997; Jain *et al*., 2000; Bollinger *et al*., 2004; Vannay *et al*., 2004; Thiede *et al*., 2005). Maintaining such high exhumation rates over 10^7 y time-scales obviously requires concomitant ongoing tectonic rock uplift in the source area.

The long-term trends in exhumation rates reported here are consistent with those inferred from detrital K-feldspar and mica $^{40}Ar/^{39}Ar$ studies on both the Siwaliks and more distal Bengal Fan deposits (Copeland & Harrison, 1990; Harrison *et al.*, 1993; Szulc *et al.*, submitted). However, in comparison to other exhumation rate estimates for the Himalaya our long-term average rate is relatively slow. For example, Burbank *et al.* (2003) used bedrock apatite FT ages to determine erosion rates of >2-5 km/Myr for the HH in the Marsyandi drainage, while Galy & France-Lanord (2001) used geochemical analyses to derive erosion rates of 2.1 – 2.9 km/Myr for the western and eastern Himalaya, respectively. Estimates on the basis of detrital white mica $^{40}Ar/^{39}Ar$ dating in western and central Nepal provide overlapping but somewhat faster exhumation rates of 1.4 – 2.0 km/Myr during the last 10 Ma (Szulc *et al.*, 2006). Therefore, our estimate could be seen as a lower limit, given that the approach we used here A) tends to average out short-term variations, which may be detected with apatite FT or (U-Th)/He and geochemical analyses, B) the closure temperature of the FT method is less than that for $^{40}Ar/^{39}Ar$ dating, therefore integrating over a shorter exhumation depth, C) our estimates are based on annealing kinetics for low-retentive α-damaged zircons

(Brandon *et al*., 1998), whereas the rapidly cooled zircons of the youngest age group may be better characterized by annealing kinetics of undamaged zircons, which may have somewhat higher closure temperatures (e.g., Rahn *et al*., 2004).

CONCLUSIONS

How can all this information be combined into one model that explains cooling and exhumation of the central Himalaya since the mid-Miocene? Considering that the Himalaya, like any other orogen, is a very complex system, the answer is most likely a combination of different tectonic, climatic, and surface processes that influenced each other and that were active at different times and different scales. We are aware that the Himalaya has a long and active history before the Miocene, but we focus here only on that part of its history that is preserved in the synorogenic sediments of the Siwalik Group and in modern river sediment. The DZFT data presented in this study provide evidence for A) widespread cooling through the zircon FT closure temperature at 16.0 ± 1.4 Ma, represented by a static peak that can be identified throughout the stratigraphic record of the Siwalik Group, B) continuous fast exhumation of deep-seated rocks at a rate of no less than 1.4 ± 0.2 km/Myr since at least 11 Ma, possibly starting as early as 15 Ma, and C) a continuous supply of recycled zircons with pre-Himalayan ZFT ages.

We think that the reoccurring ~16 Ma FT age peak is a composite peak with grains derived from different HH and LH sources that A) are related to cooling after movement on the MCT and STD, coupled with erosional exhumation, and B) are associated with cooling caused by erosion after emplacement of the Ramgarh and Dadeldhura thrust sheets onto the Lesser Himalayan units. Erosion and removal of these thrust sheets may have been enhanced by contemporaneous rapid surface uplift in the LH starting around 18 Ma. The Miocene leucogranites, on the other hand, appear to be a negligible source of zircons, even if their cooling history falls into the target age range. Relatively fast and continuous erosional exhumation of part of HH and LH rocks in the vicinity of the MCT is documented since at least 11 Ma. This exhumation is linked to continuous shortening and tectonic rock uplift, coupled to fluvial and glacial incision, as documented by dramatic relief in western and central Nepal. The old static peak of 80-150 Ma, which is present in each sample analyzed in this study, is evidence for continuous sediment recycling, most likely from non-metamorphic parts of the Tethyan Himalaya and/or now eroded sedimentary thrust sheets that were previously emplaced on top of the highly metamorphic HH, plus recycling of Tertiary foreland basin sediments.

By combining FT and U/Pb analysis on single zircon grains we were able to constrain at least general source regions for zircons deposited between 7 Ma and today (Fig. 10). Our data confirms the expectation that the Siwaliks have mainly received sediment input from the LH and HH during Miocene and Pliocene times and this signal continues in modern river sediment, even though the amount of contribution from the different lithotectonic units has changed over time, with the LH becoming an increasingly more important source with concurrent removal of HH thrust sheets. It seems that the High Himalaya has maintained its high elevation at least since the Miocene, and that the Lesser Himalaya may have experienced surface uplift after 18 Ma, given the evolution of exhumation rates determined in this study. Such surface uplift likely triggered more intense orographic precipitation, which in turn increased erosion and allowed rapid removal of parts of the HH thrust sheets on top of the Lesser Himalaya.

ACKNOWLEDGEMENTS

The European Commission supported this project through Marie Curie Postdoctoral Fellowship HPMF-CT-2002-01779 to Bernet. The INSU-CNRS “Intérieur de la Terre” program provided funding for fieldwork and analytical costs. We gratefully acknowledge constructive and supportive reviews by Andy Carter, Peter Kamp, and Hugh Sinclair, which helped to improve the quality of this paper. We also thank Jérôme Lavé for providing the “BUT” pilot samples, and F. Coeur and F. Sénébier for sample preparation and mineral separation.

REFERENCES

Ahmad, T., Harris, N., Bickle, M., Chapman, H., Bunbury, J., and Prince, C., 2000, Isotopic constraints on the structural relationships between the Lesser Himalayan Series and the High Himalayan Crystalline Series, Garhwal Himalaya: Geological Society of America Bulletin, v. 112, no. 3, p. 467-477.

Amidon, W.H., Burbank, D.W., and Gehrels, G.E., 2005a, U-Pb zircon ages as a sediment mixing tracer in the Nepal Himalaya: Earth and Planetary Science Letters, v. 235, p. 244-260.

Amidon, W.H., Burbank, D.W., and Gehrels, G.E., 2005b, Construction of detritalmineral populations: insights from mixing of U^Pb zircon ages in Himalayan rivers: Basin Research, v. 17, p. 463-485.

Appel, E., Rosler, W., and Corvinus, G., 1991, Magnetostratigraphy of the Miocene-Pliocene Surai Khola Siwaliks in west Nepal: Geophysical Journal International, v. 105, p. 191-198.

Arita, K., and Ganzawa, Y., 1997, Thrust tectonics and uplift of the Nepal Himalaya revealed from fission-track ages: Journal of Geography (Chigaku Zashi), v. 106, p. 156-167.

Batt, G.E., and Braun, J., 1997, On the thermo-mechanical evolution of compressional orogens: Geophysical Journal International, v. 128, p. 364-382.

Beaumont, C., Kooi, H., and Willett, S., 1999, Coupled tectonic-surface process models with applications to rifted margins and collisional orogens. *In* Summerfield, M.A., ed, Geomorphology and Global Tectonics, John Wiley and Sons Ltd., p. 29-55.

Beaumont, C, Jamieson, R.A., Hguyen, M.H., and Lee, B., 2001, Himalayan tectonics explained by extrusion of a low-viscosity crustal channel coupled to focused surface denudation: Nature, v. 414, p. 738-742.

Bernet, M., and Garver, J.I., 2005, Fission-track dating of detrital zircon, in Reiners, P. and Ehlers, T. editors Thermochronology, Reviews in Minerology and Geochemistry, v. 58, p. 205-238.

Bernet, M., Zattin, M., Garver, J.I., Brandon, M.T., and Vance, J.A., 2001, Steady-state exhumation of the European Alps: Geology, v. 29, p. 35-38.

Bernet, M., Brandon, M.T., Garver, J.I., and Molitor, B.R., 2004a, Downstream changes in Alpine detrital zircon fission-track ages of the Rhône and Rhine Rivers: Journal of Sedimentary Research, v. 74, p. 82-94.

Bernet, M., Brandon, M.T., Garver, J.I., and Molitor, B.R., 2004b, Fundamentals of detrital zircon fission-track analysis for provenance and exhumation studies with examples from the European Alps, *in* Bernet, M., and Spiegel, C., editors, Detrital thermochronology – exhumation and landscape evolution of mountain belts: Geological Society of America Special Publication, v. 378, p. 25-36.

Bollinger, L., Avouac, J.P., Beyssac, O., Catlos, E.J., Harrison, T.M., Grove, M., Goffe, B., and Sapkota, S., 2004, Thermal structure and exhumation history of the Lesser Himalaya in central Nepal: Tectonics, v. 23, TC5051, doi:10.1029/2003TC00156

Brandon, M.T., 1996, Probability density plot for fission track grain-age samples: Radiation Measurements, v. 26, p. 663-676.

Brandon, M.T., Roden-Tice, M.K., and Garver, J.I., 1998, Late Cenozoic exhumation of the Cascadia accretionary wedge in the Olympic Mountains, northwest Washington State: Geological Society of America Bulletin, v. 110, p. 985-1009.

Brewer, I.D., Burbank, D.W., and Hodges, K.V., 2003, Modelling detrital cooling-age populations: insights from two Himalayan catchments: Basin Research, v. 15, p. 305-320.

Brookfield, M.E., 1993, The Himalayan passive margin from Precambrian to Cretaceous times: Sedimentary Geology, v. 84, p. 1 –35.

Buiter, S. J. H., Govers, R., and Wortel, M. J. R., 2002, Two-dimensional simulations of surface deformation caused by slab detachment: Tectonophysics, v. 354, p. 195-210.

Burbank, D.W., 1996, The Himalayan foreland basin, *in* Yin, A., and Harrison, T.M., editors, The tectonics of Asia: New York, Cambridge University Press, p. 205-226.

Burbank, D.W., Blythe, A.E., Putkonen, J., Pratt-Sitaula, B., Gabet, E., Oskin, M., Barros, A., and Ojha, T.P., 2003, Decoupling of erosion and precipitation in the Himalayas: Nature, v. 426, p. 652-655.

Burchfiel, B.C., Zhilianh, C., Hodges, K.V., Yuping, L., Royden, L.H., Changrong, D., and Jiene, X., 1992, The south Tibetan detachment system, Himalayan orogen: Extension contemporaneous with and parallel to shortening in a collisional mountain belt: Geological Society of America Special Paper 269, 51p.

Carter, A., and Moss, S.J., 1999, Combined detrital-zircon fission-track and U-Pb dating: a new approach to understanding hinterland evolution: Geology, 27, p. 235-238.

Carter, A., and Bristow, C.S., 2000, Detrital zircon geochronology: enhancing the quality of sedimentary source information through improved methodology and combined U-Pb and fission-track techniques: Basin Research, 12, p. 47-57.

Carter, A., and Bristow, C.S., 2003, Linking hinterland evolution and continental basin sedimentation by using detrital zircon thermochronology: a study of the Khorat Plateau Basin, eastern Thailand: Basin Research, v. 15, p. 271-285.

Cerveny, P.F., Naeser, N.D., Zeitler, P.K., Naeser, C.W., and Johnson, N.M., 1988, History of uplift and relief of the Himalaya during the past 18 million years: Evidence from fission-track ages of detrital zircons from sandstones of the Siwalik Group, *in* Kleinspehn, K., and Paola, C., editors, New perspectives in basin analysis: New York, Springer-Verlag, p. 43-61.

Colchen, M., Le Fort, P., and Pêcher, A., 1986, Recherches geologiques dans l'Himalaya du Nepal, Annapurna; Manaslu, Ganesh Himal: Centre National de la Recherche Scientifique, Notice de la carte géologique au 1:200 000, p. 137.

Coleman, M.E., 1996, Orogen-parallel and orogen-perpendicular extension in the central Nepalese Himalayas: Geological Society of America Bulletin, v. 108, p. 1594-1607.

Copeland, P., and Harrison, T. M., 1990, Episodic rapid uplift in the Himalaya revealed by $^{40}Ar/^{39}Ar$ analysis of detrital K-feldspar and muscovite, Bengal fan: Geology, v. 18, p. 354-357.

Copeland, P., Harrison, T.M., and LeFort, P., 1990, Age and cooling of the Manaslu granite: Implications for Himalayan tectonics: Journal of Volcanology and Geothermal Research, v. 44, p. 33-50.

Copeland, P., Harrison, T.M., Hodges, K.V., Maruejol, P., LeFort, P., and Pêcher, A., 1991, An early Pliocene thermal disturbance of the Main Central thrust, central Nepal: Implications for Himalayan tectonics: Journal of Geophysical Research, v. 96, p. 8475-8500.

Corvinus, G., and Rimal, L. N., 2001, Biostratigraphy and geology of the Neogene Siwalik Group of the Surai Khola and Rato Khola areas in Nepal: Palaeogeography, Palaeoclimatology, Palaeoecology, v. 165, p. 251-279.

Crouzet, C., Stang, H., Appel, E., Schill, E., and Gautam, P., 2001, Detailed analysis of successive pTRMs carried by pyrrhotite in Himalayan metacarbonates: an example from Hidden Valley, Central Nepal: Geophysical Journal International, v. 146, p. 607-618.

Deloule, E., Alexandrov, P., Cheilletz, A., Laumonier, B. and Barbey, P., 2002, In-situ U-Pb zircon ages for Early Ordovician magmatism in the eastern Pyrenees, France: the Canigou orthogneisses: International Journal of Earth Sciences, v. 91, p. 398-405.

Deniel, C., Vidal, P., Fernandez, A., LeFort, P., and Peucat, J.J., 1987, Isotopic study of the Manaslu granite (Himalaya Nepal): Inferences on the age and source of Himalayan leucogranites: Contributions to Mineralogy and Petrology, v. 96, p. 78-92.

DeCelles, P.G., Gehrels, G.E., Quade, J., Ojha, T.P., Kapp, P.A., and Upreti, B.N., 1998, Neogene foreland basin deposits, erosional unroofing, and kinematic history of the Himalayan fold-thrust belt, Nepal: Geological Society of America Bulletin, v. 110, p. 2-21.

DeCelles, P.G., Gehrels, G.E., Quade, J., LaReau, B., and Spurlin, M. 2000, Tectonic implications of U–Pb zircon ages of the Himalayan orogenic belt in Nepal: Science, v. 288, p. 497– 499.

DeCelles, P. G., Robinson, D. M., Quade, J., Ojha, T. P., Garzione, C. N., Copeland, P., and Upreti, B. N., 2001, Stratigraphy, structure, and tectonic evolution of the Himalayan fold-thrust belt in western Nepal: Tectonics, v. 20, p. 487-509.

DeCelles, P.G., Gehrels, G.E., Najman, Y., Martin, A.J., Carter, A., and Garzanti, E., 2004, Detrital geochronology and geochemistry of Cretaceous-Early Miocene strata of Nepal: Implications for timing and diachroneity of initial Himalayan orogenesis: Earth and Planetary Science Letters, v. 227, p. 313-330.

Ferrara, G., Lombardo, B., and Tonarini, S., 1983, Rb/Sr geochronology of granites and gneisses from the Mount Everest region, Nepal Himalaya, Geologische Rundschau, v. 72, p. 119– 136.

France-Lanord, C., Derry, L., and Michard, A., 1993, Evolution of the Himalaya since Miocene time: Isotopic and sedimentologic evidence from the Bengal Fan, *in* Treloar, P. J., and Searle, M., eds., Himalayan tectonics: Geological Society [London] Special Publication, v. 74, p. 603–621.

Galbraith, R.F., and Green, P.F., 1990, Estimating the component ages in a finite mixture: Nuclear Tracks and Radiation Measurements, v. 17, p. 197–206.

Galy, A., and France-Lanord, C., 2001, Higher erosion rates in the Himalaya: Geochemical constrains on riverine fluxes: Geology, v. 29, p. 23-26.

Gansser, A., 1964, Geology of the Himalayas: London, Interscience, 289 p.

Garver, J.I., and Brandon, M.T., 1994, Erosional denudation of the British Columbia Coast Ranges as determined from fission-track ages of detrital zircon from the Tofino Basin, Olympic Peninsula, Washington: Geological Society of America Bulletin, v. 106, p.1398-1412.

Garver, J.I., Brandon, M.T., Roden-Tice, M. K., and Kamp, P. J. J., 1999, Exhumation history of orogenic highlands determined by detrital fission track thermochronology, *in* Ring, U., and others, editors, Exhumation Processes: Normal faulting, Ductile Flow, and Erosion: Geological Society [London] Special Publications, v. 154, p. 283-304.

Garver, J. I., Brandon, M.T., Bernet, M., Brewer, I., Soloviev, A.V., Kamp. P.J.J., and Meyer, N., 2000, Practical consideration for using detrital zircon fission track thermochronology for provenance, exhumation studies, and dating sediments, The ninth International Conference of Fission-track dating and Thermochronology, Lorne Australia. Geological Society of Australia Abstract Series, v. 58, p. 109-111.

Garver, J.I., Reiners, P.W., Walker, L.J., Ramage, J.M., and Perry, S.E., 2005, Implications for timing of Andean uplift from thermal resetting of radiation damaged zircon in the Cordillera Huayhuash, Northern Peru: Journal of Geology, v. 113, p. 117-138.

Garzanti, E., Gorza, M., Martellini, L., and Nicora, A., 1994, Transition from diagenesis to metamorphism in the Paleozoic to Mesozoic succession of the Dolpo-Manang Synclinorium and Thakkhola Graben (Nepal Tethys Himalaya): Eclogae Geologicae Helveticae, v. 87, no. 2, p. 613-632.

Gautam, P., and Rösler, W., 1999, Depositional chronology and fabric of Siwalik Group sediments in central Nepal from magnetostratigraphy and magnetic anisotropy: Journal of Asian Earth Sciences, v. 17, p. 659-682.

Gautam, P., and Fujiwara, Y., 2000, Magnetic polarity stratigraphy of Siwalik Group sediments of Karnali River section in western Nepal: Geophysical Journal International, v. 142, p. 812-824.

Grujic, D., Hollister, L. S., and Parrish, R. R., 2002, Himalayan metamorphic sequence as an orogenic channel: insight from Bhutan: Earth and Planetary Science Letters, v. 198, p. 177-191.

Guillot, S., Hodges, K., Le Fort, P., and Pêcher, A., 1994, New constraints on the age of the Manaslu leucogranite: Evidence for episodic tectonic denudation in the central Himalaya: Geology, v. 22, p. 559-562.

Harrison, T.M., Copeland, P., Kidd, W.S.F., and Yin, A., 1992, Raising Tibet: Science, v. 255, p. 1663-1670.

Harrison, T. M., Copeland, P., Hall, S. A., Quade, J., Burner, S., Ojha, T. P., and Kidd, W. S. F., 1993, Isotopic preservation of Himalayan/Tibetan uplift, denudation, and climatic histories in two molasse deposits: Journal of Geology, v. 100, p. 157-173.

Hodges, K. V., 2000, Tectonics of the Himalaya and southern Tibet from two perspectives: Geological Society of America Bulletin, v. 112, p. 324-350.

Hodges, K. V., Parrish, R. R., and Searle, M. P., 1996, Tectonic evolution of the central Annapurna Range, Nepalese Himalayas: Tectonics, v. 15, p. 1264–1291.

Hodges, K. V., Hurtado, J. M., and Whipple, K. X., 2001, Southward extrusion of Tibetan crust and its effect on Himalayan tectonics: Tectonics, v. 20, p. 799-809.

Hubbard, M.S., and Harrison, T.M., 1989, $^{40}Ar/^{39}Ar$ constraints on deformation and metamorphism in the Main Central thrust zone and Tibetan slab, eastern Nepal Himalaya: Tectonics, v. 8, p. 865-880.

Hurford, A.J., 1986, Cooling and uplift patterns in the Lepontine Alps, South Central Switzerland and an age of vertical movement on the Insubric fault line: Contributions to Mineralogy and Petrology, v. 92, p. 413-427.

Hurford, A.J., 1998, Zeta: The ultimate solution to fission-track analysis calibration or just an interim measure? *In* Van den Haute, P, and De Corte, F., eds., Advances in Fission-Track Geochronology, p. 19-32.

Huyghe, P., Galy, A., Mugnier, J-L., and France-Lanord, C., 2001, Propagation of the thrust system and erosion in the Lesser Himalaya: Geochemical and sedimentological evidence: Geology, v. 29, p. 1007-1010.

Huyghe, P., Mugnier, J. L., Gajurel, A. P., and Delcaillau, B., 2005, Tectonic and climatic control of the changes in the sedimentary record of the Karnali River section (Siwaliks of Western Nepal): The Island Arc, v.14, p 311-327.

Jain, A. K., Kumar, D., Singh, S., Kumar, A., and Lal, N., 2000, Timing, quantification and tectonic modelling of Pliocene-Quaternary movements in the NW Himalaya: evidence from fission track dating: Earth and Planetary Science Letters, v. 179, p. 437-451.

Kohn, M.J., Catlos, E.J., Ryerson, F.J., and Harrison, T.M., 2001, Pressure-temperature-time path discontinuity in the Main Central thrust zone, central Nepal: Geology, v. 29, p. 571-574.

LeFort, P., 1975, Himalaya: the collided range. Present knowledge of the continental arc: American Journal of Science, v. 275, no. A, p. 1-44.

LeFort, P., 1981, Manaslu leucogranite: A collision signature of the Himalaya: A model for its genesis and emplacement: Journal of Geophysical Research, v. 86, p. 10545–10568.

LeFort, P., 1986, Metamorphism and magmatism during the Himalayan collision, *in* Coward, M. P., and Ries, A. C., eds., Collision tectonics: London, Geological Society Special Publication 19, p. 159–172.

Macfarlane, A.M., 1993, Chronology of tectonic events in the crystalline core of the Himalaya, Langtang National Park: Tectonics, v. 12, p. 1004-1025.

Macfarlane, A.M., Hodges, K.V., and Lux, D., 1992, A structural analysis of the Main Central thrust zone, Langtang National Park, central Nepal Himalaya: Geological Society of America Bulletin, v. 104, p. 1389-1402.

Molnar, P., England, P., and Martinod, J., 1993, Mantle dynamics, uplift of the Tibetan Plateau, and the Indian monsoon: Reviews of Geophysics, v. 31, p. 357-396.

Mugnier, J. L., Mascle, G., and Faucher, T., 1993, Structure of the Siwaliks of western Nepal: An intracontinental accretionary prism: International Geology Reviews, v. 35, p. 32–47.

Mugnier, J. L., Huyghe, P., Leturmy, P., and Jouanne, F., 2004, Episodicity and rates of thrust sheet motion in Himalaya (western Nepal), *in* McClay, K.R., ed., Thrust tectonics and hydrocarbon systems: American Association of Petroleum Geologists Memoir 82, p. 91-114.

Mugnier, J. L., and Huyghe, P., 2006, The Ganges Basin geometry records a pre-15 Ma isostatic rebound of Himalaya: Geology, v. 34, p. 445-448.

Naeser, N.D., Zeitler, P.K., Naeser, C.W., and Cerveny, P.F., 1987, Provenance studies by fission track dating–etching and counting procedures: Nuclear Tracks and Radiation Measurements, v. 13, p. 121-126.

Najman, Y., 2006, The detrital record of orogenesis: A review of approaches and techniques used in the Himalayan sedimentary basins: Earth-Science Reviews, v. 74, p. 1-72.

Nakata, T., 1989, Active faults of the Himalaya of India and Nepal, *in* Malinconico, L. L., Jr., and Lillie, R. J., eds., Tectonics of the western Himalayas: Geological Society of America Special Paper 232, p. 243–264.

Nakayama, K., and Ulak, P., 1999, Evolution of fluvial style in the Siwalik Group in the foothills of the Nepal Himalaya: Sedimentary Geology, v. 125, p. 205-224.

Parrish, R. R., and Hodges, K. V., 1996, Isotopic constraints on the age and provenance of the Lesser and Greater Himalayan sequences, Nepalese Himalaya: Geological Society of America Bulletin, v. 108, p. 904–911.z

Pearson, O.N., and DeCelles, P.G., 2005, Structural geology and regional tectonic significance of the Ramgarh thrust, Himalayan fold-thrust belt of Nepal: Tectonics, v. 24, TC4008, doi:10.1029/2003TC001617.

Pêcher, A., 1975, The Main Central Thrust of the Nepal Himalaya and the related metamorphism in the Modi-Khola cross-section (Annapurna Range), Himalayan Geology, v. 5, p. 115 – 132

Pêcher, A., 1989, The metamorphism in the central Himalaya: Journal of Metamorphic Geology, v. 7, p. 31–41.

Quade, J., Cater, J. M. L., Ojha, T. P., Adam, J., and Harrison, T. M., 1995, Late Miocene environmental change in Nepal and the northern Indian subcontinent: Stable isotopic evidence from paleosols: Geological Society of America Bulletin, v. 107, p. 1381–1397.

Rahn, M. K., Brandon, M. T., Batt, G. E., and Garver, J. I., 2004, A zero-damage model for fission track annealing in zircon: American Mineralogist, v. 89, p. 473–484.

Raymo, M. W., and Ruddiman, W. F., 1992, Tectonic forcing of late Cenozoic climate: Nature, v. 359, p. 117-122.

Robinson, D.M., DeCelles, P.G., Patchett, P.J., and Garzione, C.N., 2001, The kinematic history of the Nepalese Himalaya interpreted from Nd isotopes: Earth and Planetary Science Letters, v. 192, p. 507–521.

Robinson, D.M., DeCelles, P.G., Garzione, C.N., Pearson, O.N., Harrison, T.M., and Catlos, E.J., 2003, Kinematic model for the Main Central thrust in Nepal: Geology, v. 31, p. 359-362.

Ruhl, K.W., and Hodges, K.V., 2005, The use of detrital mineral cooling ages to evaluate steady state assumptions in active orogens: An example from the central Nepalese Himalaya: Tectonics, v. 24, TC4015, doi:10.1029/2004TC001712.

Ruiz, G. M. H., Seward, D., and Winkler, W., 2004, Detrital thermochronology - a new perspective on hinterland tectonics, an example from the Andean Amazon Basin, Ecuador: Basin Research, v. 16, no. 3, p. 413-430.

Sakai, H., Takigami, Y., Nakamuta, Y., and Nomura, H., 1999, Inverted metamorphism in the Pre-Siwalik foreland basin sediments beneath the crystalline nappe, western Nepal Himalaya: Journal of Asian Earth Sciences, v. 17, p. 727-739.

Schärer, U., Xu, R. H., and Allègre, C. J., 1986, U-(Th)-Pb systematics and ages of Himalayan leucogranites, south Tibet: Earth and Planetary Science Letters, v. 77, p. 35–48.

Schelling, D., 1992, The tectonostratigraphy and structure of the eastern Nepal Himalaya: Tectonics, v. 11, p. 925–943.

Searle, M. P., Noble, S. R., Hurford, A. J., and Rex, D. C., 1999, Age of crustal melting, emplacement and exhumation history of the Shivling leucogranite, Garhwal Himalaya: Geological Magazine, v. 136, p. 513-525.

Searle, M. P., and Godin, L, 2003, The Tibetan Detachment and the Manaslu Leucogranite: A structural reinterpretation and Restoration of the Annapurna-Manaslu Himalaya, Nepal. Journal of Geology, v. 111, p. 505-523.

Spiegel, C., Kuhlemann, J., Dunkl, I., Frisch, W., von Eynatten, H., and Balogh, K., 2000, The erosion history of the Central Alps: evidence from the zircon fission-track data of the foreland basin sediments: Terra Nova, 12, p. 163-170.

Stacey, J.S. and Kramers, J.D., 1975, Approximation of tererstrial lead isotope evolution by a two-stage model: Earth and Planetary Science Letters, v. 26, p. 207-221.

Stephenson, B. J., Waters, D. J, and Searle, M.P., 2000, Inverted metamorphism and the Main Central Thrust: Field relations and thermobarometric constraints from the Kishtwar Window, NW Indian Himalaya, Journal of Metamorphic Geology, v. 18, p. 571 – 590.

Stewart, R. J., and Brandon, M. T., 2004, Detrital-zircon fission-track ages for the "Hoh Formation": Implications for late Cenozoic evolution of the Cascadia subduction wedge: Geological Society of America Bulletin, v. 116, no. 1, p. 60-75.

Stöcklin, J., 1980, Geology of Nepal and its regional frame: Geological Society of London Journal, v. 137, p. 1–34.

Stüwe, K., White, L., and Brown, R., 1994, The influence of eroding topography on steady-state isotherms: Application to fission track analysis: Earth and Planetary Science Letters, v. 124, p. 63-74.

Szulc, A. G., Najman, Y., Sinclair, H., Pringle, M., Bickle, M., Chapman, H., Garzanti, E., Ando, S., Huyghe, P., Mugnier, J. L., Ojha, T. P., and DeCelles, P. G., 2006, Tectonic evolution of the Himalaya constrained by a detrital investigation of three Siwalik foreland basin successions, SW Nepal: Basin Research v. 18, p. XXX-XXX.

Thiede, R. C., Arrowsmith, J. R., Bookhagen, B., McWilliams, M. O., Sobel, E. R., and Strecker, M. R., 2005, From tectonically to erosionally controlled development of the Himalayan orogen: Geology, v. 33, no. 8, p. 689-692.

Upreti, B. N., 1999, An overview of the stratigraphy and tectonics of the Nepal Himalaya: Journal of Asian Earth Sciences, v. 17, no. 5-6, p. 577-606.

Valdiya, K. S., 1980, Geology of the Kumaon Lesser Himalaya: Wadia Institute of Himalayan Geology, 291 p.

van der Beek, P.A., Robert, X., Mugnier, J.L., Bernet, M., Labrin, E., and Huyghe, P., 2006, Late Miocene – Recent denudation of the central Himalaya and recycling in the foreland basin assessed by detrital apatite fission-track thermochronology of Siwalik sediments, Nepal, Basin Research, v. 18, p. XXX-XXX.

Vannay, J.-C., Grasemann, B., Rahn, M., Frank, W., Carter, A., Baudraz, V., and Cosca, M., 2004, Miocene to Holocene exhumation of metamorphic crustal wedges in the NW Himalaya: Evidence for tectonic extrusion coupled to fluvial erosion: Tectonics, v. 23, p. TC1014, doi:10.1029/2002TC001429.

Von Eynatten, H., and Wijbrans, J.R., 2003, Precise tracing of exhumation and provenance using $^{40}Ar/^{39}Ar$ geochronology of detrital white mica: the example of the central Alps. In McCann, T., and Saintot, A., eds., Tracing Tectonic Deformation Using the Sedimentary Record: Geological Society, London, Special Publications, v. 208, p. 289-305.

Wagner, G., and Van den haute, P., 1992, Fission-track dating. Solid Earth Sciences Library, Kluwer Academic Publishers, 285p.

West, R. M., Lukacs, J. R., Munthe, J., and Hussain, T., 1978, Vertebrate fauna from Neogene Siwalik Group, Dang valley, western Nepal: Journal of Paleontology, v. 52, p. 1015–1022.

White, N.M., Pringle, M., Garzanti, E., Bickle, M, Najman, Y., Chapman, H., and Friend, P., 2002, Constraints on the exhumation and erosion of the High Himalayan Slab, NW India, from foreland basin deposits: Earth and Planetary Science Letters, v. 195, p. 29-44.

Wiedenbeck, M., Allé, P., Corfu, F., Griffin, W.L., Meier, M., Oberli, F., Von Quadt, A., Roddick, J.C. and Spiegel W., 1995, Three natural zircon standards for U-TH-Pb, Lu-Hf, trace elements and REE analyses: Geostandards Newsletter, v. 19, p. 1-23.

Willett, S., 1999, Orogeny and orography: The effects of erosion on the structure of mountain belts: Journal of Geophysical Research, v. 104. p. 28,957-28,981.

Willett, S, and Brandon, M.T., 2002, On steady states in mountain belts: Geology, v. 30, p. 175-178.

Yin, A., and Harrison, T. M., 2000, Geologic Evolution of the Himalayan-Tibetan Orogen: Annual Review of Earth and Planetary Sciences, v. 28, no. 1, p. 211-280.

FIGURE CAPTIONS

Fig. 1 Simplified geologic map of Nepal showing major lithotectonic units and fault systems (modified from DeCelles *et al.*, 2004). Locations of the Karnali, Surai Khola, and Tinau Khola sample sites are marked with a star, the LH samples BIR 1 and SUR 23 are marked with crosses.

Fig. 2 Generalized stratigraphic section of the Siwalik Group in western Nepal giving short facies descriptions and depositional environments (based on own observations and DeCelles *et al.*, 1998). Shown are also the stratigraphic locations of the samples analyzed in this study.

Fig. 3 A) General lag-time concept as it is used in DZFT analysis, using a simplified vertical exhumation path. Abbreviations: t_c = time of closure, t_e = time of erosion, t_d = time of deposition. Time for erosion and transport is negligible in active orogenic systems and therefore geologically instantaneous. Consequently lag time is defined as t_c-t_d. B) Example of a synthetic probability density plot. Given are binomial best-fit peaks as they may be derived from an orogen shown in A. C) Three principle lag-time trends that may be observed in DZFT peak ages from a suite of samples collected from a stratigraphic profile.

Fig. 4 Probability density plot of DZFT results of the Karnali River in western Nepal. Shown are the observed grain-age distribution in form of a histogram and in curve form (stippled line). The curve is the same as a continuous histogram. Also shown is the binomial best-fit solution with 4 peaks at 4, 9, 19 and > 200 Ma.

Fig. 5 Lag-time plot of DZFT peak ages of Siwaliks Group (Karnali, Surai Khola, and Tinau Khola sections combined), and modern river sediment. Note that lag-time contours are curved in both plots because of the logarithmic scale used for the FT age axis. Peak ages are given with 2 sigma errors.

Fig. 6 Results of DZFT analysis of samples from sedimentary units in the Lesser Himalaya, located in proximity to the MBT. The data indicate a group of fully reset low retentive zircon with cooling ages ~15 Ma, and partially or non-reset zircons with much older FT ages. See text and Garver *et al.* (2005) for further discussion of low retentive zircon.

Fig. 7 Double-dating results of combined FT and U/Pb analysis on single zircons. Shown are 61 grains selected from samples KAR-UP, SUR20, SUR17, and SUR8 (Table 3). The symbols indicate the different samples, grey scale shows to which of the three peaks the grains belong. FT age errors are given at the 2 sigma level. The combination of the two dating techniques allows differentiation between TH, HH and LH. Frequency curve of Himalayan detrital zircon U/Pb ages compiled from DeCelles *et al.* (2004) and references therein.

Fig. 8 Concordia plot for U/Pb ages of zircon that were dated with the FT and U/Pb method. All U/Pb ages were determined with an Cameca IMS 1270 ion microprobe at the CRPG in Nancy.

Fig. 9 No direct zircon FT ages exist for the Manaslu leucogranite, but based on other thermochronologic data by Deniel *et al.* (1987), Copeland *et al.* (1990) and Guillot *et al.* (1994) the cooling rate of the Manaslu leucogranite in eastern Nepal can be determined, which allows estimation of the approximate zircon FT cooling age of ~16 Ma for the Miocene intrusions.

Fig. 10 Simplified cross-sections through western Nepal showing the structural evolution of the Himalaya during the Miocene-Present. Given are generalized lithotectonic units and major fault systems, as well as potential zircon FT and U/Pb source terrains (modified from Huyghe *et al.*, 2005). U/Pb ages compiled from DeCelles *et al.* (1998, 2000, 2004) and Hodges *et al.* (1996); present-day ZFT ages compiled from Arita & Ganzawa (1997), Jain *et al.* (2000), and Vannay *et al.* (2004). Not shown are potential zircon sources in the Tethyan Himalayas which have ZFT of about 100 Ma and U/Pb ages of mainly 400-1200 Ma (DeCelles *et al.*, 1998, 2000, 2004).

TABLES

Table 1 Detrital zircon fission-track data of the Karnali River, Tinau Khola, and Surai Khola sections

Table 2 Zircon fission-track data of Lesser Himalayan sedimentary samples

Table 3. Zircon U/Pb data

Table 1: Detrital zircon FT data of the Karnali, Surai Kohla, and Tinau Kohla section

Samples	deposition (Ma)	*n*	Age range (Ma)	moving peak	young static peak	old static peak	other peaks
Karnali							
KA-up	0	64	1.8 – 201.2	4.0 ± 1.1 17.6%	19.1 ± 3.0 34.6%	216.6 ± 135.7 1.6%	9.3 ± 1.3 46.2%
KAR-12	6.0	30	8.2 – 121.5		15.9 ± 1.7 79.5%	106.0 ± 32.5 20.5%	
KAR-7	10.9	11	7.8 – 138.6	No peaks fitted			
KAR-6	12.1	37	7.9 – 182.6	16.5 ± 2.2 64.9%		85.7 ± 16.2 35.1%	
KAR-3	14.1	24	12.9 – 215.6	18.7 ± 3.2 67.5%		99.2 ± 27.5 32.5%	
Surai Khola							
RAP	0.0	27	4.8 – 20.7	4.9 ± 3.5 3.8%	13.8 ± 1.4 96.2%		
SUR-20	1.0	27	3.5 – 425.5	5.4 ± 1.4 34.0 %	13.5 ± 3.3 37.5%	114.0 ± 37.8 28.5%	
SUR-19	3.1	69	4.3 – 240.5	7.6 ± 1.5 31.1%	14.1 ± 2.2 39.9%	109.7 ± 20.0 29.0%	
SUR-17	4.0	40	3.7 – 168.4	6.2 ± 1.2 44.8%	15.4 ± 3.1 35.2%	93.6 ± 24.2 20.0%	
SUR-16	4.0	40	4.6 – 219.4	8.5 ± 1.6 41.5%	18.8 ± 3.3 33.3%	98.1 ± 28.5 25.2%	
SUR-15	4.8	29	6.3 – 158.5	10.8 ± 1.5 61.9 %		91.8 ± 20.8 38.1%	
SUR-1	4.9	35	6.3 – 116.2	10.9 ± 2.1 46.6%	17.5 ± 3.8 36.3%	88.4 ± 26.5 17.1%	
SUR-3	5.0	68	7.0 – 352.8	13.6 ± 3.3 48.9%	17.5 ± 5.7 37.8%	108.1 ± 25.3 13.3%	
SUR-8	7.0	46	4.8 - 270.1	11.8 ± 2.1 45.8%	19.4 ± 3.3 36.6%	102.2 ± 27.4 17.6%	
SUR-12	11.0	28	8.6 – 140.2	14.4 ± 1.6 82.1%		81.3 ± 24.4 17.9%	
SUR-13	12.0	40	10.5 – 208.6		18.3 ± 1.9 75.1%	83.3 ± 18.1 24.9%	
Tinau Khola							
BUT5	6.3	32	7.2 – 198.6	10.1 ± 1.6 23.3%	18.4 ± 1.7 57.9%	90.7 ± 17.7 18.7%	
TIN-8	7.9	21	10.5 – 147.9		14.6 ± 1.7 90.2%	120.1 ± 82.1 9.8%	
BUT4+TA5	9.1	45	7.2 – 236.3	8.9 ± 3.4 8.5%	16.1 ± 1.9 53.1%	129.3 ± 23.2 38.4%	
TIN-5	10.3	53	7.5 – 230.1	15.6 ± 1.5 81.1%		107.9 ± 28.2 18.9%	
TA14	10.5	17	8.3 – 256.5	14.2 ± 1.5 76.5%		88.8 ± 23.4 23.5%	
BUT2+TA18	10.9	42	8.0 – 287.5	13.0 ± 2.3 39.1%	23.9 ± 4.0 37.5%	158.8 ± 38.5 23.4%	

Note: *n* = total number of grains counted; binomial peak-fit ages are given ±2 SE. Also given is the percentage of grains in a specific peak. All samples were counted at 1250x dry (100x objective, 1.25 tube factor, 10 oculars) by M. Bernet using a zeta (CN-1) of 126.71 ± 5.36 (±1 SE). Samples BUT 5, TA5, TA14 and TA18 were dated by E. Labrin (CN-1 zeta 142.2 ± 3.21). Depositional ages after Gautam and Fujiwara (2000) for the Karnali River section, and T.P. Ohja (pers. commun. 2003) for the Surai and Tinau sections..

Table 2: Fission-track data of the Lesser Himalayas sedimentary samples

Samples	Formation	*n*	Age range (Ma)	P1	P2
BIR 1	Dumri Fm.	13	12.1 – 92.5	15.6 ± 3.0 69.2%	79.9 ± 27.6 30.8%
SUR 23	Khamari Fm	14	9.8 – 66.8	14.5 ± 2.5 71.4%	53.0 ± 13.5 28.6%

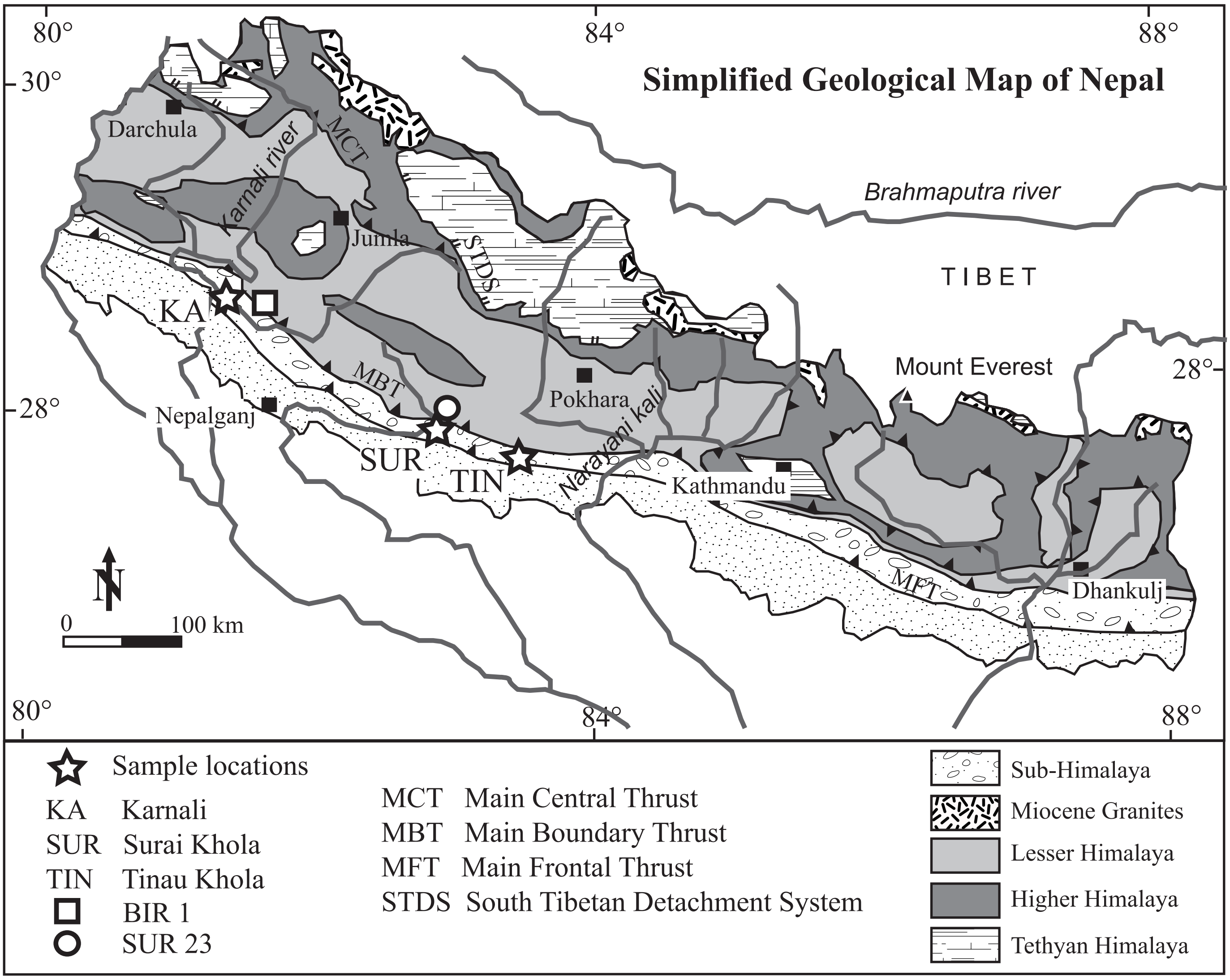

Fig. 1 Bernet et al.

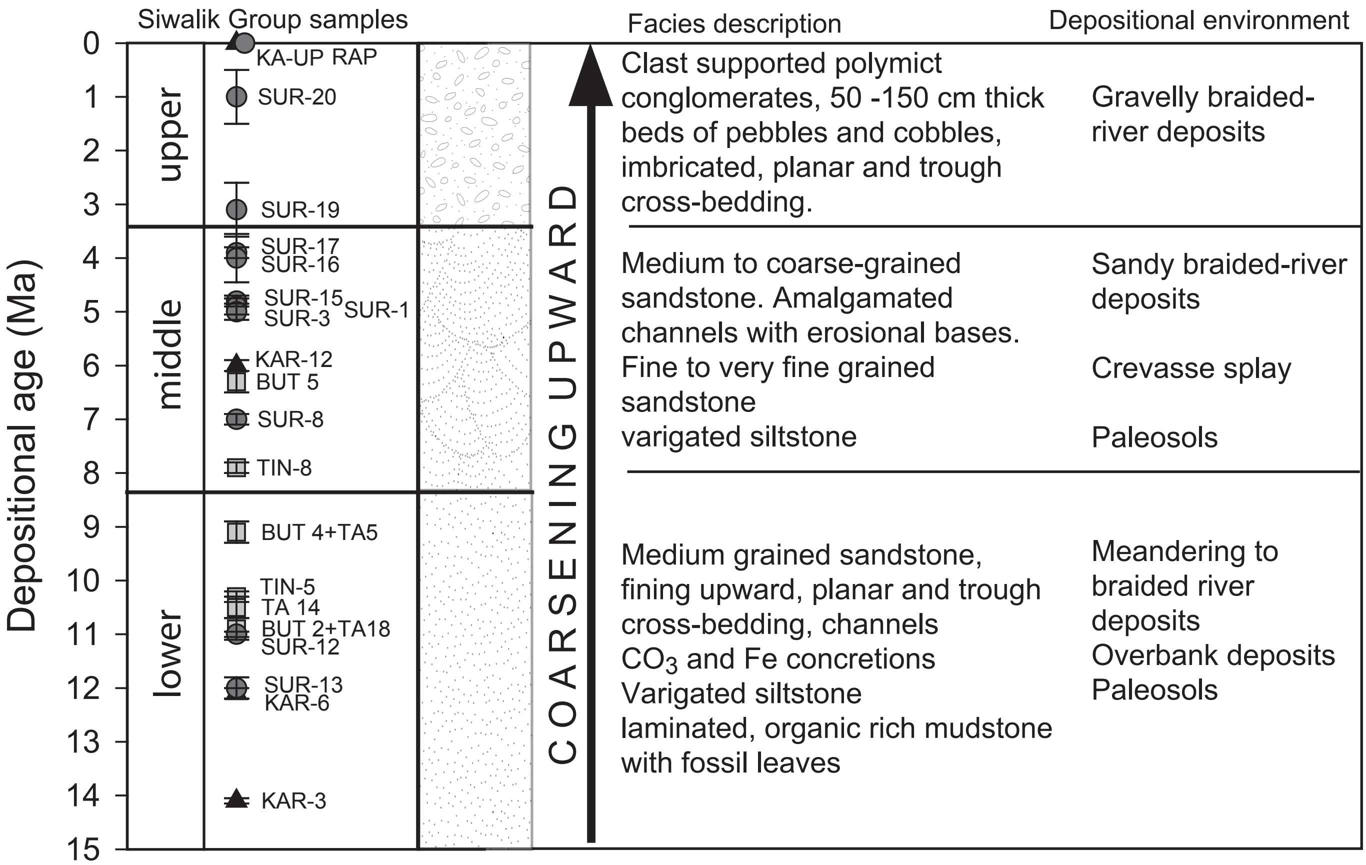

Fig. 2 Bernet et al.

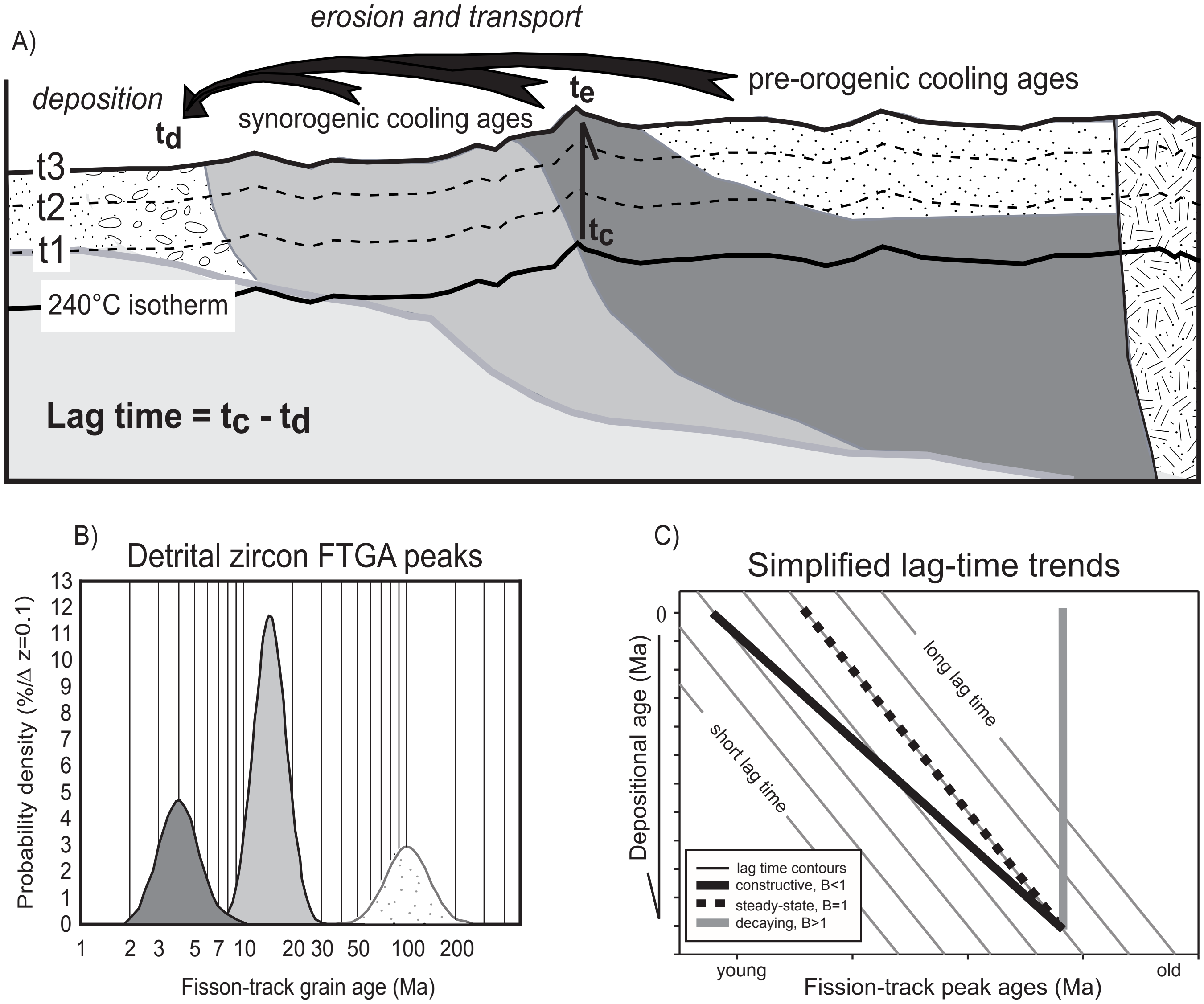

Fig. 3 Bernet et al.

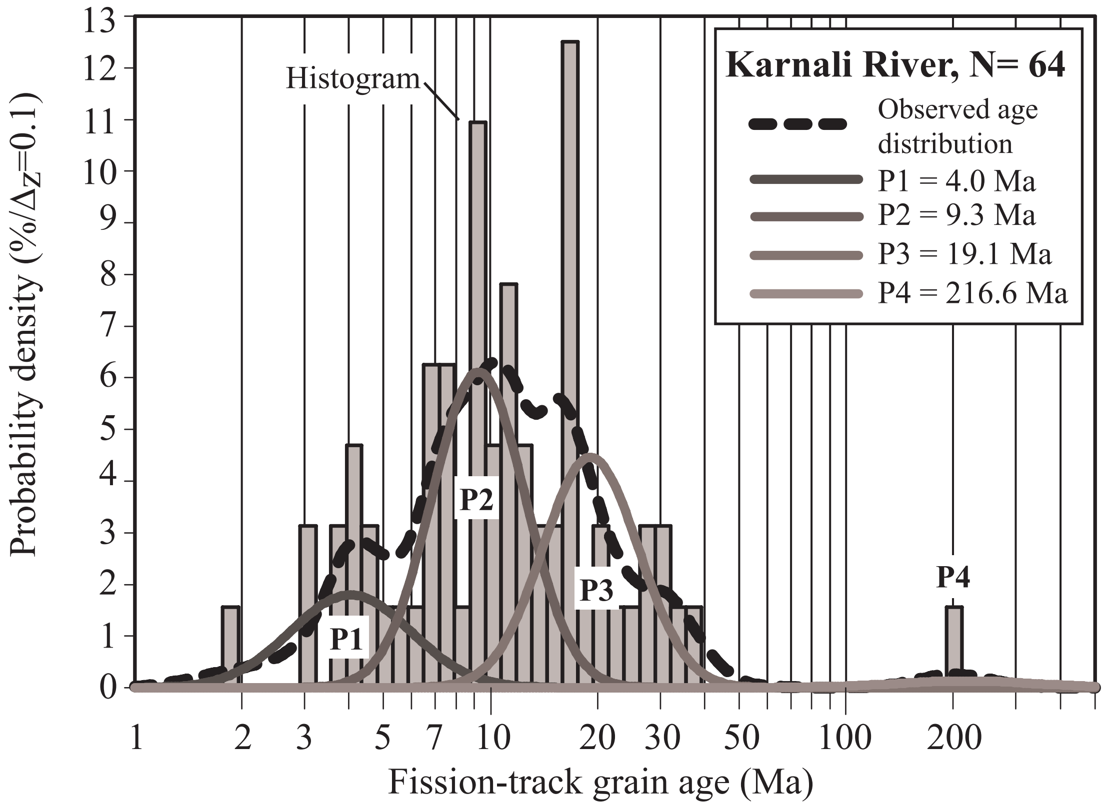

Fig. 4 Bernet et al.

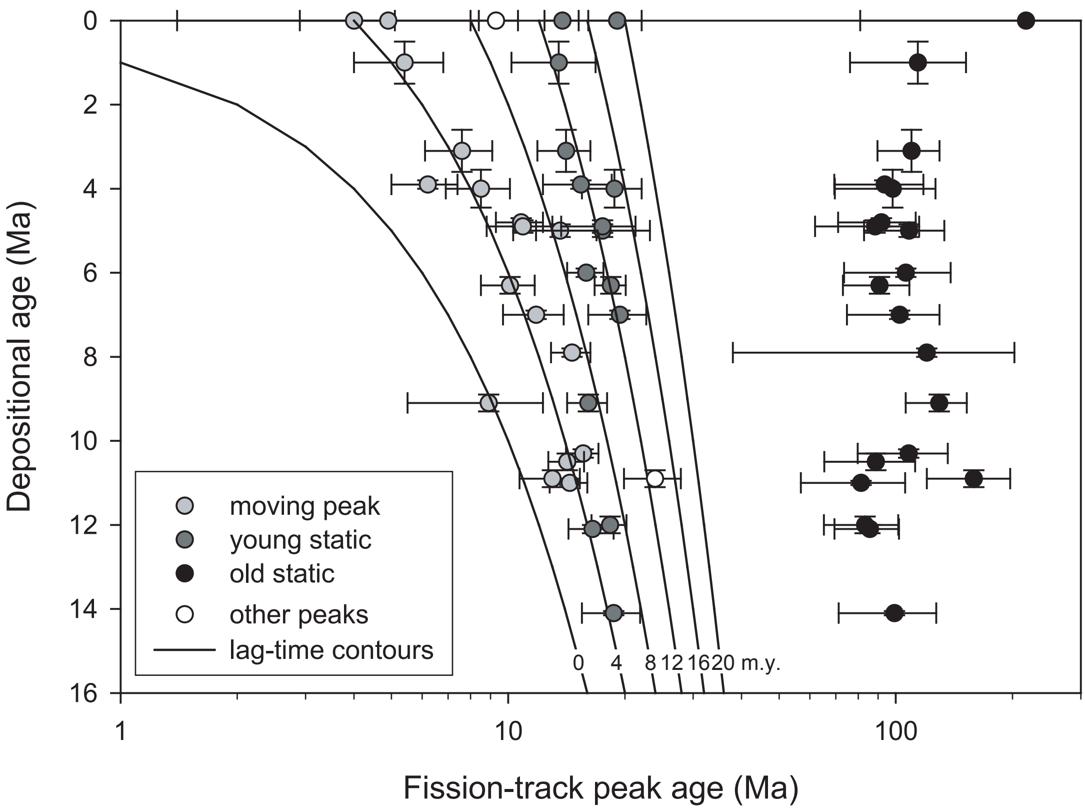

Fig. 5 Bernet et al.

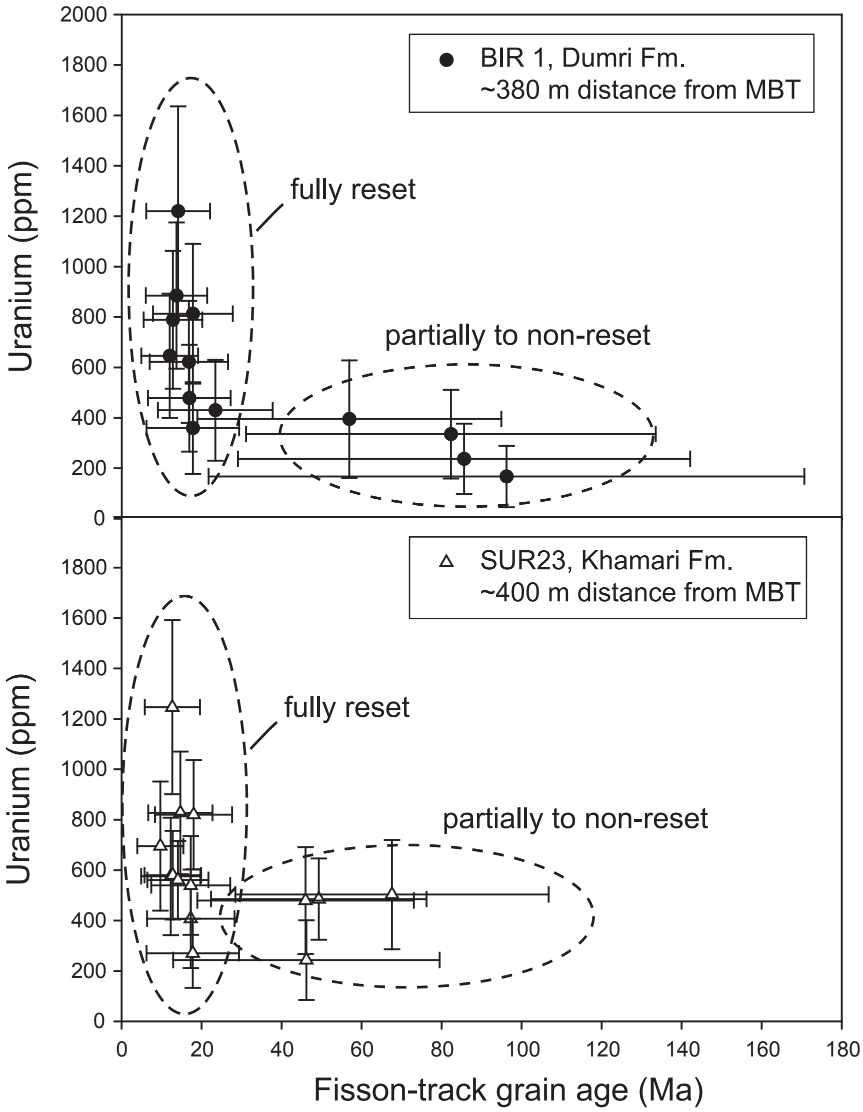

Fig. 6 Bernet et al.

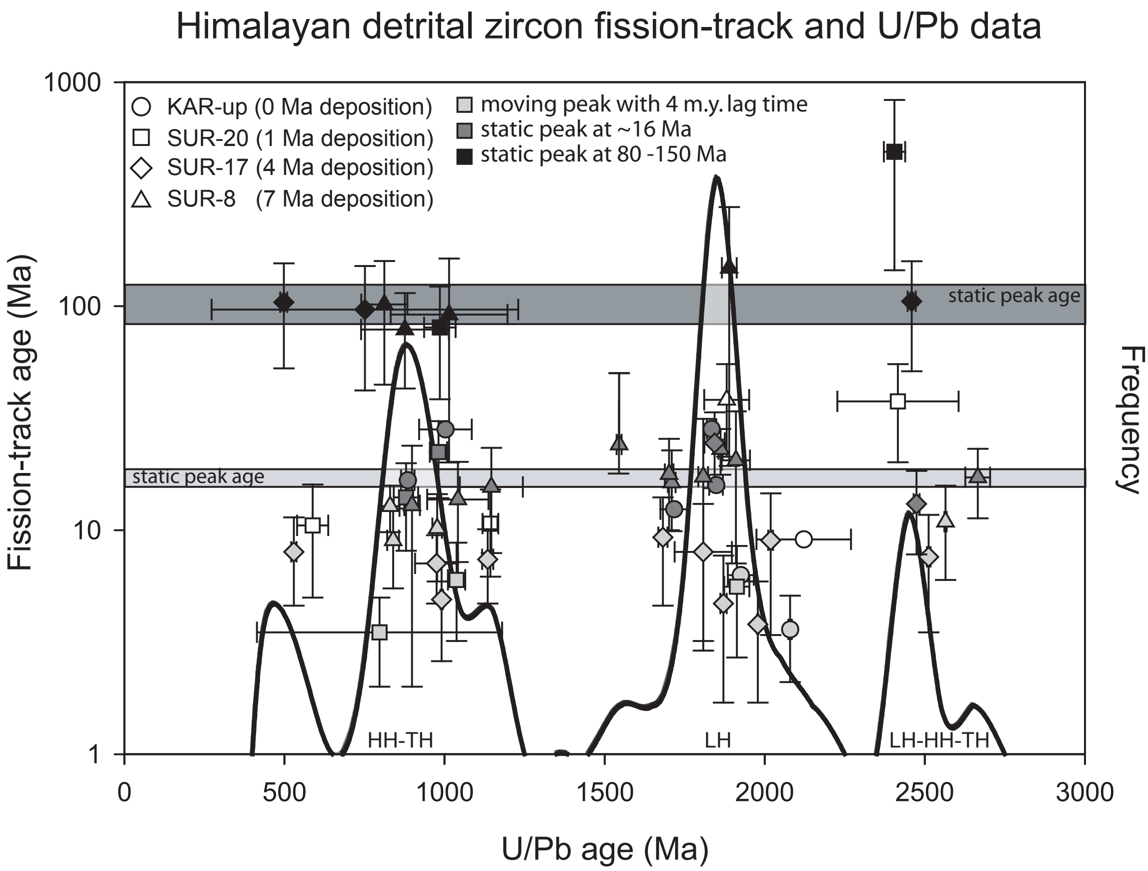

Fig. 7 Bernet et al.

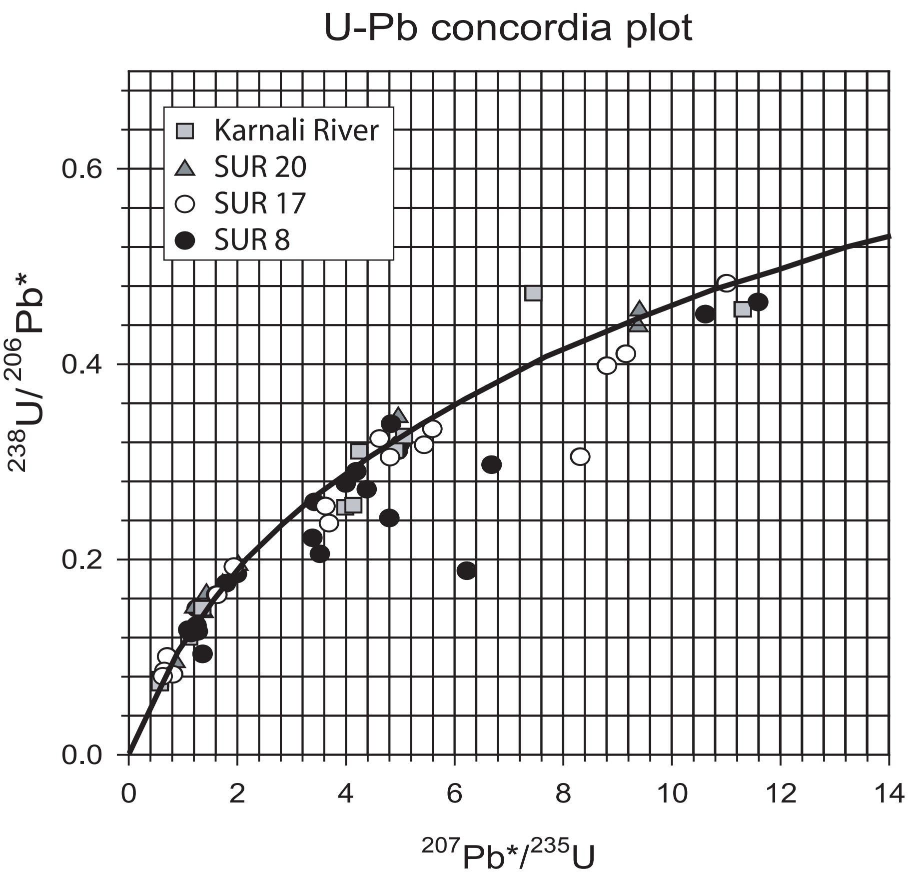

Fig. 8 Bernet et al.

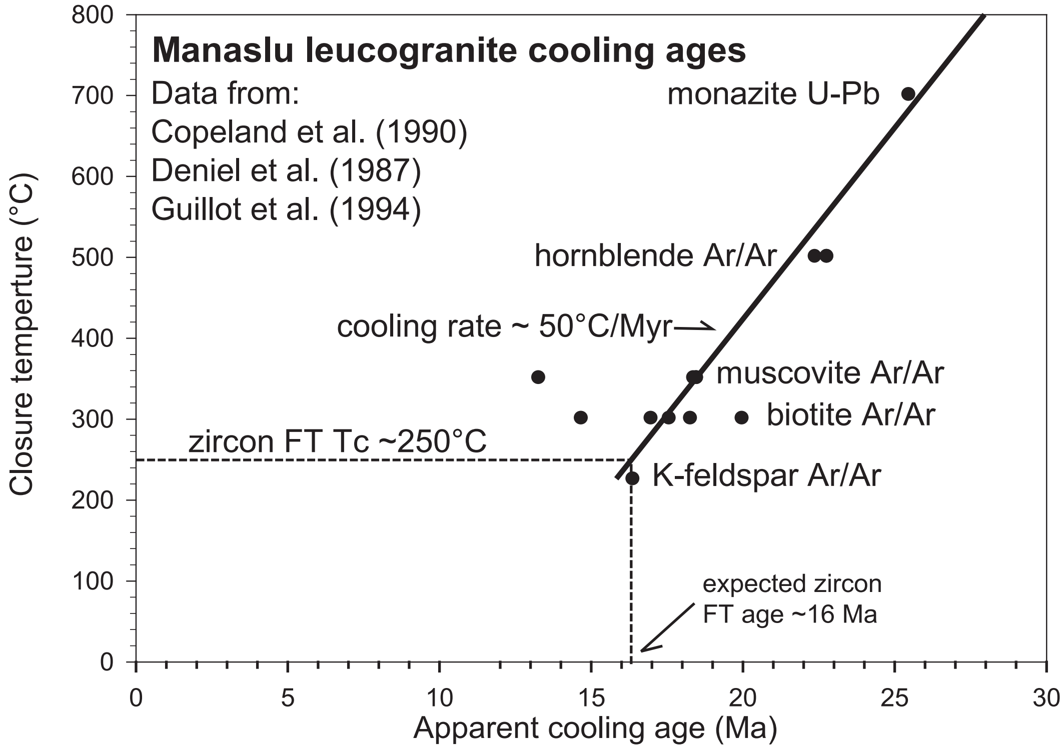

Fig. 9 Bernet et al.

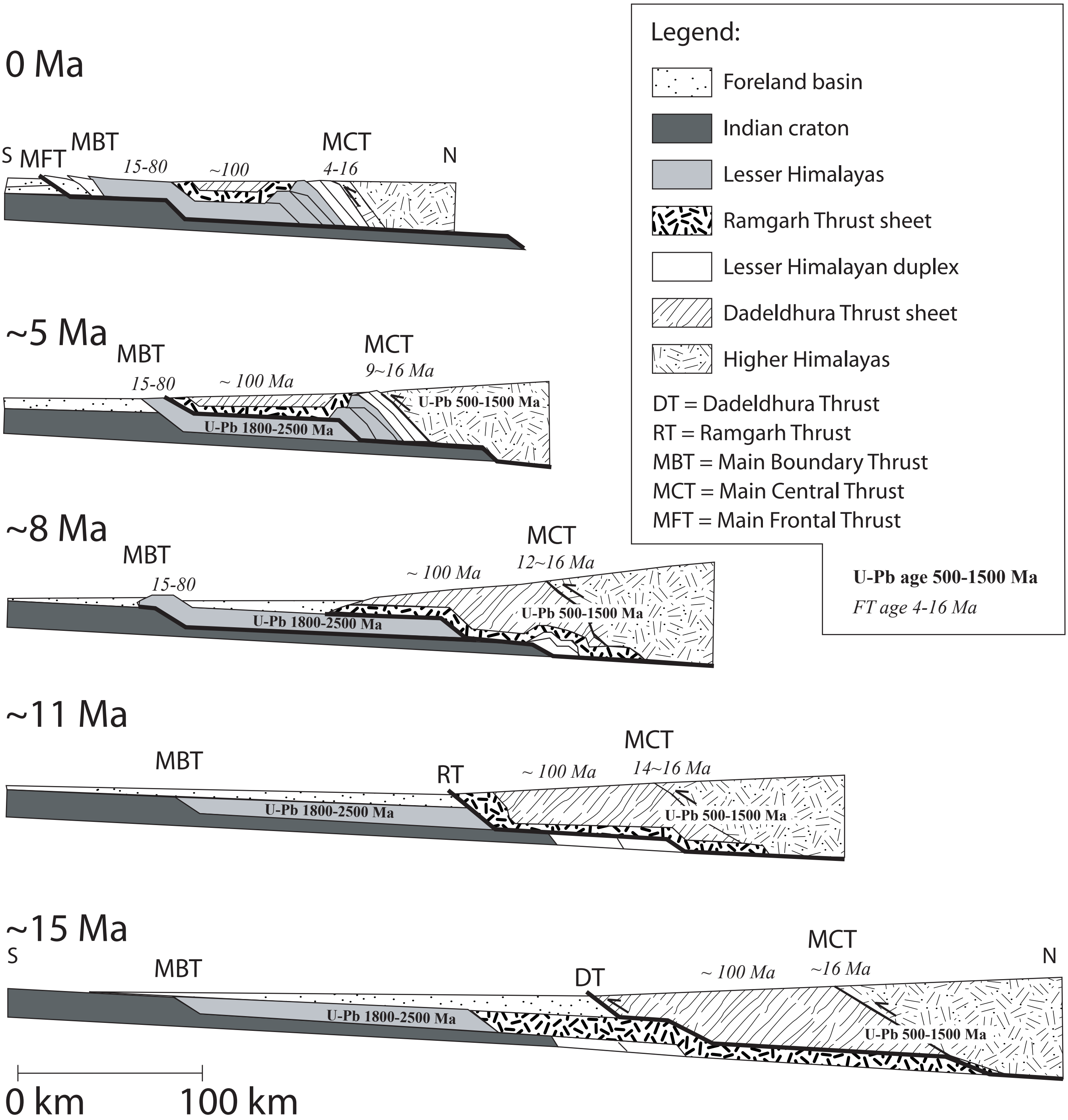

Figure 10 Bernet et al.